



University of  
Massachusetts  
Amherst

## Role of Manganese Oxide in the Formation of Disinfection Byproducts in Drinking Water Treatment

Item Type	Dissertation (Open Access)
Authors	Bazilio, Arianne A.
DOI	<a href="https://doi.org/10.7275/11248296.0">10.7275/11248296.0</a>
Download date	2026-03-06 09:27:02
Link to Item	<a href="https://hdl.handle.net/20.500.14394/17341">https://hdl.handle.net/20.500.14394/17341</a>

Role of Manganese Oxide in the Formation of Disinfection Byproducts in Drinking  
Water Treatment

A Dissertation Presented

by

ARIANNE A. BAZILIO

Submitted to the Graduate School of the  
University of Massachusetts Amherst in partial fulfillment  
of the requirements for the degree of

DOCTOR OF PHILOSOPHY

February 2018

Department of Civil and Environmental Engineering

© Copyright by Arianne A. Bazilio 2018

All Rights Reserved

Role of Manganese Oxide in the Formation of Disinfection Byproducts in Drinking  
Water Treatment

A Dissertation Presented

by

ARIANNE A. BAZILIO

Approved as to style and content by:

---

John E. Tobiason, Chair

---

David A. Reckhow, Member

---

Wei Fan, Member

---

Richard N. Palmer, Department Head  
Civil and Environmental Engineering Department

To my parents, Allan and Anjie Bazilio.

## ACKNOWLEDGEMENTS

I would like to sincerely thank my advisor, Dr. Tobiason, for his support and mentorship over the years. I have greatly benefited from your seemingly endless knowledge of water treatment (and many other things), and am a better researcher and critical thinker because of your tutelage. I would also like to thank Dr. Fan and Dr. Reckhow for serving on my committee and providing valuable input and feedback. Thank you Dr. Reckhow for mentoring and advising me from my time as an MS student to today, and serving on numerous committees over the years.

I would like acknowledge various funding sources: Aquarion Water Company of Connecticut, AAUW, and NEWWA. A special thank you to employees at AWC plants I have worked with over the years, and especially to Gary Kaminski and Yesher Larsen.

Thank you Sherrie Webb-Yagodzinski for everything you do, and Chuyên for spending many of your summer hours helping me in the lab. Thanks to my colleagues and friends, especially Xuyen, Will, Varun, Rassil, Vivek, Mike, and Aarthi who contributed in some way to my work. To my friends who supported me through this crazy journey: Ashwini, Edwina, Angela, Judy, Aditi, Melody, Sabrina, Jackie, Daunette, and Carolina. Thank you Suzanne for keeping me physically able to do lab work, and making me feel at home during a very stressful time. To my family, thank you from the bottom of my heart for your endless support, especially Auntie Desiree, Auntie Shivaun, and Uncle Lynden. Allana and Adrian, you're the best siblings ever; thank you for supporting me well into adulthood. And finally, to my parents: here's to the irony of me being the doctor in the family. Thank you for patiently supporting me throughout my education, and making sacrifices so that I could get where I am today.

## ABSTRACT

### ROLE OF MANGANESE OXIDE IN THE FORMATION OF DISINFECTION BYPRODUCTS IN DRINKING WATER TREATMENT

FEBRUARY 2018

ARIANNE A. BAZILIO, B.S., NEW YORK UNIVERSITY

M.S., UNIVERSITY OF MASSACHUSETTS AMHERST

Ph.D., UNIVERSITY OF MASSACHUSETTS AMHERST

Directed by: Professor John E. Tobiason

This work examined the role of manganese oxide ( $MnO_x$ ) in the formation of disinfection byproducts (DBPs) in drinking water treatment. DBPs are of increasing concern as more is being learned about their carcinogenicity and genotoxicity. Studies were performed to determine the impact of  $MnO_x$  and free chlorine ( $Cl_2$ ), used for dissolved manganese (Mn(II) removal, on the formation of these undesirable byproducts.

Batch experiment results showed that the presence of  $MnO_x$  did not significantly increase the haloacetic acid or trihalomethane concentrations. Rates of DBP formation were also similar in the absence and presence of Mn(II) at the beginning of the reaction. The purported reason for similar DBP concentrations is that aquatic natural organic matter (NOM) does not readily adsorb to  $MnO_x$  under the conditions (pH, time, etc.) typical of drinking water treatment plants (WTPs).

Results of column studies were consistent with batch results; exposure to  $MnO_x$  coated granular filter media did not increase DBP formation. Measured instantaneous DBP concentrations were higher when  $Cl_2$  was applied ahead of the column as compared to after the column. However, measured DBP concentrations when all samples were held for 24 hours were similar. The practice of only post-filter chlorination is not feasible for

WTPs with the treatment goal of removing Mn(II) across a MnO<sub>x</sub>-coated granular media filter.

An alternative method which allows the post-filtration application of Cl<sub>2</sub> while removing Mn(II) by sorption and catalytic oxidation by Cl<sub>2</sub> is employing second stage contactors (SSCs) solely for Mn(II) removal. This decoupling of particle (and NOM) and Mn(II) removal was documented at the full-scale at a newly reconstructed direct filtration WTP. The SSCs successfully removed Mn(II), and a substantial decrease in DBP formation was observed. There was no measurable increase in DBP formation across the SSCs.

# TABLE OF CONTENTS

	Page
ACKNOWLEDGEMENTS .....	v
ABSTRACT .....	vi
LIST OF TABLES .....	x
LIST OF FIGURES .....	xi
<b>CHAPTER</b>	
<b>1. OVERVIEW AND INTRODUCTION .....</b>	<b>1</b>
<b>2. DBP FORMATION IN THE PRESENCE AND ABSENSE OF MANGANESE DIOXIDE.....</b>	<b>4</b>
2.1 Introduction .....	4
2.2 Materials and Methods .....	7
2.2.1 Chemicals.....	7
2.2.2 Manganese Oxide Synthesis .....	7
2.2.3 Mn(II) and NOM Adsorption Experiments .....	8
2.2.4 DBP Formation and Kinetic Experiments .....	9
2.2.5 Analysis.....	10
2.2.6 Particle and Media Characterization .....	11
2.3 Results .....	12
2.3.1 Characterization .....	12
2.3.2 Mn(II) and NOM Adsorption .....	13
2.3.3 DBP Formation .....	17
2.3.4 Kinetic Studies .....	22
2.4 Conclusions .....	27

**3. IMPACT OF MANGANESE OXIDE-COATED GRANULAR FILTER MEDIA ON DISINFECTION BYPRODUCT FORMATION .....28**

3.1 Introduction .....28

3.2 Materials and Methods .....31

    3.2.1 Column Experiments .....31

        3.2.1.1 Column Setup.....31

        3.2.1.2 Granular Media .....33

        3.2.1.2 Column Influent.....33

    3.2.2 Full Scale Experiments .....35

    3.2.3 Analysis.....36

3.3 Results .....36

    3.3.1 Column Study Water Quality Parameters.....36

    3.3.2 Column Study Disinfection Byproduct Formation .....38

    3.3.3 Full Scale Disinfection Byproduct Formation .....41

        3.3.3.1 Putnam WTP .....41

        3.3.3.2 Lantern Hill WTP .....47

3.4 Conclusions .....51

**4. FULL-SCALE IMPLEMENTATION OF SECOND-STAGE CONTACTORS FOR MANGANESE REMOVAL .....53**

4.1 Introduction .....53

4.2 Materials and Methods .....58

    4.2.1 The Full Scale Plant .....58

    4.2.2 Field Sampling .....60

    4.2.3 Analytical Methods .....62

        4.2.3.1 Field Measurements .....62

        4.2.3.2 Laboratory Measurements .....62

    4.2.4 Media and Backwash Particle Characterization .....62

4.3 Results .....63

4.3.1 Dual Media Filtration: Turbidity, Iron and NOM Removal .....	64
4.3.2 Disinfection Byproducts .....	66
4.3.3 Second Stage Contactors.....	69
4.3.3.1 Mn Removal.....	69
4.3.3.2 Contactor Backwash .....	70
4.3.3.3 Mn Mass Balance.....	71
4.3.3.4 Media and Backwash MnO <sub>x</sub> Characterization .....	73
4.3.4 Broader Treatment Implications .....	77
4.3 Conclusions .....	77
<b>5. CONCLUSIONS .....</b>	<b>79</b>
APPENDICES	
A. SUPPLEMENTAL DATA FOR CHAPTER 2 .....	82
B. SUPPLEMENTAL DATA FOR CHAPTER 3.....	83
BIBLIOGRAPHY.....	85

## LIST OF TABLES

Table	Page
2.1: HAA <sub>5</sub> and TTHM concentrations using ~ 0.5 g/L MnO <sub>x</sub> particles in presence or absence of Cl <sub>2</sub> and/or Mn(II). Reaction time 5 hours, residual Cl <sub>2</sub> ~1 mg/L, ~ 4 mg/L DOC, where present 0.55 mg/L Mn(II), at pH 6.1 ± 0.2. ....	22
3.1: Summary of Putnam WTP raw water quality from January 2014 to December 2016. ....	33
3.2: Water quality parameters at the time of collection of Putnam settled water. ....	34
3.3: Summary of column effluent water quality parameters for different runs. ....	37
3.4: Average instantaneous HAA <sub>5</sub> concentrations and percentages. ....	41
3.5: Average instantaneous TTHM concentrations and percentages. ....	43
3.6: Average 24-hour DBP concentrations and percentage differences. ....	46
3.7: Average instantaneous HAA <sub>5</sub> concentrations and percentages. ....	47
3.8: Average instantaneous TTHM concentrations and percentages. ....	48
3.9: Average 24-hour DBP concentrations and percentage differences. ....	49
B.1: Column run water quality parameters. ....	83

## LIST OF FIGURES

Figure	Page
2.1: SEM image of synthesized MnO <sub>x</sub> particles (magnification 20,000X). .....	13
2.2: Mn(II) adsorption isotherm and modeled Langmuir fit at pH 5.1 using a 20 mg/L MnO <sub>x</sub> suspension at room temperature. ....	14
2.3: NOM adsorption isotherms for different ionic strengths and Ca <sup>2+</sup> concentrations. pH 6.1 using a 0.5 g/L MnO <sub>x</sub> suspension at ~20 °C for 24 ± 1 hours; 5mM carbonate buffer, 0.5 mM Ca <sup>2+</sup> .....	16
2.4: Change in dissolved organic carbon concentration and Mn(II) evolution at high ionic strength (50 mM NaCl) in the presence of Ca <sup>2+</sup> ions (0.5 mM) and 0.5 g/L MnO <sub>x</sub> . .....	16
2.5: (a) HAA <sub>5</sub> and (b) TTHM concentrations over time using ~4 mg/L DOC, residual Cl <sub>2</sub> ~ 1mg/L after 6 hours, and coated or uncoated granular media at pH 6.9 ± 0.2. ....	18
2.6: HAA <sub>5</sub> formation for different initial DOC concentrations after 4 hours at pH 6.1 ± 0.2, residual Cl <sub>2</sub> ~ 1mg/L, with 0.5 g/L MnO <sub>x</sub> or no MnO <sub>x</sub> . ....	19
2.7: (a) HAA <sub>5</sub> and (b) TTHM concentrations formed when NOM was chlorinated with no media, uncoated or coated media present. Reaction time 5 hours, residual Cl <sub>2</sub> ~0.5 mg/L, ~ 4 mg/L DOC, UV <sub>254</sub> 0.14 cm <sup>-1</sup> , where present 0.55 mg/L Mn(II), at pH 6.0 ± 0.2. ....	20
2.8: (a) TCAA and (b) DCAA concentrations over time with and without 0.55 mg/L Mn(II). Approximately 0.5 g/L MnO <sub>x</sub> , ~3.5 mg/L DOC, pH 6.3 ± 0.2, ~2 mg/L residual Cl <sub>2</sub> . ....	23
2.9: Linear region of (a) TCAA and (b) DCAA formation. ....	24
2.10: HAA <sub>5</sub> and DBCM concentrations overtime using a clarified surface water. MnO <sub>x</sub> concentration 0.5 g/L, pH 6.5, [Mn(II)] = 0.30 mg/L, DOC = 2.1 mg C/L. ....	26
3.1: Schematic of column setup. ....	32
3.2: Schematic of Putnam WTP (adapted from 2017 Putnam Report). ....	35
3.3: Sample (a) instantaneous and (b) 24 hour HAA <sub>5</sub> concentrations. ....	39
3.4: Sample (a) instantaneous and (b) 24 hour BDCM concentrations. ....	40

3.5: Average (a) HAA <sub>5</sub> and (b) TTHM concentrations of filter influent and effluent samples held for 24 hours. * indicates that pre-oxidation with chlorine dioxide was in use at the time of sample collection. ....	45
3.6: Average (a) HAA <sub>5</sub> and (b) TTHM concentrations of SSC influent and effluent samples held for 24 or 48 hours. *indicates that samples were held for 48 hours.....	50
4.1: Schematic of reconstructed LHWTP. ....	59
4.2: Iron fractionation across the plant on August 27th, 2013.....	65
4.3: Contactor to waste Mn and residual chlorine concentrations post DM filter backwash on November 11th, 2013.....	66
4.4: Plant Effluent DBP concentrations from 2010 to 2015. ....	67
4.5: Instantaneous across the plant, and 24 and 48 hr. SDS DBP concentrations on August 29th, 2013. ....	68
4.6: Manganese fractionation across the plant on August 27th, 2013. ....	70
4.7: Cumulative mass of Mn removed and in backwash from July 2013 to September 2015.....	72
4.8: SSC media MnOx coating depth profiles (a) February 2014 (b) September 2015. ..	74
A.1: Adsorbed and solution organic carbon concentrations. Reaction time 24 hours, pH of 6.1, at 20 °C, 0.5 mM Ca <sup>2+</sup> .. ....	82
B.1: Instantaneous TTHM concentrations.....	83

## CHAPTER 1

### OVERVIEW AND INTRODUCTION

The oxidation of dissolved manganese (Mn(II)) present in drinking water is responsible for operational and aesthetic problems in the treatment plant and distribution system. Dissolved Mn is typically removed by oxidation (with a strong oxidant such as permanganate, chlorine dioxide, or ozone) prior to particle removal, or by sorption on a manganese oxide (MnO<sub>x</sub>) coated media surface.

In the United States, chlorine is commonly used as a disinfectant in drinking water treatment, making it a convenient choice for Mn(II) oxidation. However, free chlorine reacts at a very slow rate with Mn(II), relative to typical plant hydraulic retention times, at pH less than about 8.5. The slow rate of Mn(II) oxidation by free chlorine is circumvented by sorption of Mn (II) to a MnO<sub>x</sub> surface, such as coated granular media, followed by oxidation by free chlorine. This process occurs rapidly (on the order of seconds), effectively removing Mn(II) from water (Knocke, Occiano and Hungate (1991)).

Some of the disinfection byproducts (DBPs) formed when disinfectants used in water treatment react with bromide and/or natural organic matter present in the source water are now known to be carcinogenic and genotoxic (Richardson et al. (2007a)). There are several classes of DBPs, some of which are currently regulated by the US Environmental Protection Agency (EPA). Regulations are becoming more stringent, and the number of regulated compounds will potentially be increased. The application of free chlorine just prior to granular media filtration, as practiced for Mn (II) removal by sorption and catalytic oxidation, was previously shown to significantly increase DBP

formation as compared to chlorine application to the same water after granular media filtration (Corbin et al. (2003)).

Many studies have shown that aquatic natural organic matter (NOM) adsorbs to metal oxide surfaces, including manganese oxides, primarily by complex formation between the hydroxyls and acidic functional groups of NOM and the metal oxide surface (Day et al. (1994)). One study (Gallard et al. (2009)) found that the manganese oxide birnessite facilitated the formation of iodinated organic compounds (including iodoform) when NOM and iodide were present in water. However, free chlorine was not used in the study. Previous work at UMass Amherst on chlorination prior to granular media filtration both at full-scale (Warner WTP, CT) and bench-scale (anthracite/sand column filters, clarified water from Warner WTP) indicated that there was accumulation of DBP precursors as particulate NOM built up on filter media over the course of a filter run and the precursors can react with chlorine. Eliminating pre-filter chlorine eliminated the reaction (Brown et.al. 2006).

The purpose of this research was to investigate the role of manganese oxide as a catalyst in DBP formation in drinking water treatment. While many have studied its role as a catalyst in the removal of dissolved manganese in treatment, there has not been a study that examines the role of  $MnO_x$  as a catalyst in the reaction between natural organic matter and free chlorine in the formation of halogenated disinfection byproducts. With stricter disinfection byproduct regulations possible in the future, it is important to explore this subject since many drinking water treatment plants with dissolved manganese in their source water use free chlorine and oxide coated media for Mn(II) removal. The potential impact of manganese oxide on resulting DBP concentrations has important implications

in the design and operation of drinking water treatment plants for the removal of dissolved manganese.

**CHAPTER 2**  
**DBP FORMATION IN THE PRESENCE AND ABSENCE OF MANGANESE**  
**DIOXIDE**

**2.1 Introduction**

Manganese (Mn) in drinking water sources usually occurs at concentrations lower than the lifetime health advisory of 0.3 mg/L suggested by the U.S. Environmental Protection Agency (USEPA) (USEPA (2004)). Surveys of Mn in drinking water supplies reported mean values ranging from 2 - 32  $\mu\text{g/L}$  (0.002 - 0.032 mg/L) (US Agency for Toxic Substances and Disease Registry (2012)). However, results from a study by Bouchard et al. (2011) found that intellectual impairment in children aged 6-13 was associated with exposure to Mn levels common in groundwater.

Dissolved manganese (Mn(II) or  $\text{Mn}^{2+}$ ) is typically removed during drinking water treatment to avoid operational problems and consumer complaints. The recommended treatment goal to avoid chronic problems is 0.02 mg/L Mn (Brandhuber et al. (2013)), lower than the secondary maximum contaminant level (SMCL) of 0.05 mg/L recommended by the USEPA to avoid aesthetic problems (USEPA (1992)).

In the conventional treatment of surface waters where Mn(II) removal is an objective, removal is often achieved across coated granular filter media with pre-filter chlorination. The Mn(II) in the water sorbs to the manganese oxide ( $\text{MnO}_x$ , where x may vary from 1.3 to 2) coated surface and is then oxidized by free chlorine ( $\text{HOCl}$  and  $\text{OCl}^-$ ). This catalytic oxidation reaction is very fast (on the order of seconds to minutes) compared to the much slower rate of oxidation of Mn(II) by  $\text{HOCl}$  in solution at pH less than approximately 8.5 (Knocke, Occiano and Hungate (1991)). An alternative method is

to have second stage contactors (after filtration) containing coarse  $\text{MnO}_x$  coated media for Mn(II) adsorption and catalytic oxidation by HOCl (Knocke et al. (2010); Bazilio et al. (2016)).

Chlorine may react with natural organic matter (NOM) present in source waters to form halogenated organic disinfection byproducts (DBPs), some of which are currently regulated by the USEPA. However, unregulated DBPs may be more carcinogenic and genotoxic than those currently regulated (Richardson et al. (2007b)). Exposure to DBPs has been linked to increased risk of colon, bladder, and rectum cancers (Sayess et al. (2017); Villanueva, C.M., Cantor, K.P., Grimalt, J.O., Malats, N., Silverman, D., Tardon, A., Garcia-Closas, R., Serra, C., Carrato, A., Castano-Vinyals, G. and Marcos, R. (2007); Bull et al. (1995)). The practice of pre-filter chlorination for Mn(II) removal has been shown to increase DBP formation compared to comparable post-filtration chlorination that is implemented for primary disinfection (Corbin et al. (2003)). One possible explanation for the increased DBP formation could be that the  $\text{MnO}_x$  catalyzes the reaction between NOM and HOCl, in addition to the desired reaction between Mn(II) and HOCl.

Gallard et al. (2009) showed that  $\text{MnO}_x$  catalyzed the formation of iodinated organics, such as iodoform, when iodide and NOM were present in the reaction matrix.  $\text{MnO}_x$  acted as both a catalyst and oxidizing agent for proposed reactions occurring in the system. Other research (Wang and Stone (2006a); Wang and Stone (2006b); Ulrich and Stone (1989); Stone and Morgan (1984a); Stone and Morgan (1984b)) showed that  $\text{MnO}_x$  oxidized some organic compounds, including catechols, hydroquinones, and resorcinols (model DBP precursors). Some of the organics oxidized in the studies contain functional

groups similar to those found in NOM. While numerous studies have shown that  $\text{MnO}_x$  can oxidize certain organic compounds, those experiments were conducted in the absence of a solution phase oxidant such as chlorine.

The properties of the  $\text{MnO}_x$  are also important.  $\text{MnO}_x$  used in most studies to date were not similar to the  $\text{MnO}_x$  coating that develops on granular media in drinking water treatment. Characterization of media from filters used for Mn(II) removal showed more amorphous manganese oxides (Merkle et al. (1996); Islam et al. (2010); Bazilio et al. (2016)) than the  $\text{MnO}_x$  used in most bench-scale studies. A study of the impact of crystallinity on the pH of the zero point of charge (pH(ZPC)) of Mn(IV) oxides found that the pH(ZPC) increased from 1.5 for the amorphous  $\delta$  form to 7.3 for the most well-defined crystalline form ( $\beta$ -  $\text{MnO}_2$  (Pyrolusite)). The pH at which the surface becomes negatively charged increases, and the surface area decreases, with increasing crystallinity (Healy, Herring and Fuerstenau (1966)). Mn(II) adsorption to  $\text{MnO}_x$  increases with increasing pH, and the adsorption of negatively charged species would be expected to be low at pH above the pH(ZPC) of the  $\text{MnO}_x$ .

In a study of the oxidation of citrate by  $\text{MnO}_2$ , Wang and Stone (2006a) proposed an autocatalytic scheme resulting from two parallel processes, the relatively slow oxidation of free citrate by surface  $\text{Mn}^{3+,4+}$ , and the concerted reaction of resulting  $\text{Mn}^{2+}$ -citrate complexes with surface  $\text{Mn}^{3+,4+}$ , both producing  $\text{Mn}^{2+}$  and citrate oxidation products. Adding Mn(II) eliminated the observed initial induction period, and had minimal impacts on the maximum reaction rate ( $r_{\text{max}}$ ) at low concentration, and decreasing  $r_{\text{max}}$  to a much smaller extent than another cation ( $\text{Zn}^{2+}$ ) at high concentrations. The mechanism for the proposed scheme involved metal-to-metal

electron transfer from  $\text{Mn}^{2+}$ -citrate to surface  $\text{Mn}^{3+,4+}$ , generating  $\text{Mn}^{3+}$ -citrate complexes which are transformed by intramolecular electron transfer.

The impact of  $\text{MnO}_x$  on the reaction between NOM and chlorine to form halogenated organic DBPs when chlorine and NOM are present as for Mn(II) removal by sorption and catalytic oxidation is not understood. This research aimed to determine whether the presence of  $\text{MnO}_x$  increased the formation of DBPs when NOM and free chlorine were present in solution. Batch experiments were performed with  $\text{MnO}_x$  particles and  $\text{MnO}_x$  coated granular media under different experimental conditions, and the resulting DBP formation was evaluated.

## **2.2 Materials and Methods**

### **2.2.1 Materials**

All chemicals used were reagent grade or purer. Where available, reagents with > 99.99 % purity on a trace metal basis were used. Deionized Millipore-Mili Q (18  $\Omega$ W) Ultrapure water produced by a Milli-Q system (Millipore) was used for all experiments. Suwanee River NOM (RO isolate 2R101N) was purchased from the International Humic Substances Society.

### **2.2.2 Manganese Oxide Synthesis**

Manganese oxide ( $\text{MnO}_x$ ) particles were synthesized by precipitation from solution after a method developed by Murray (1974). Permanganate (Mn in the +7 oxidation state) was used to oxidize Mn(II) to Mn(IV) oxides, and the Mn(VII) was itself reduced to Mn(IV) oxides (Equation 2.1).



Potassium permanganate (approximately 1 g) was added to a 4 L Erlenmeyer flask with approximately 3.5 L ultrapure water. A stoichiometric amount of manganese (II) sulfate monohydrate (approximately 1.5 g) was dissolved in approximately 500 mL of ultrapure water, and this solution was added dropwise to the permanganate solution which was stirred rapidly using a Teflon coated stir bar and a magnetic stirring plate. A 5% or 10% (wt/wt%) sodium hydroxide solution was added dropwise to neutralize the acid produced by the reaction and to keep the pH between 6 - 7. These steps were repeated several times, and the particles were allowed to settle and were rinsed with ultrapure water until the 0.2  $\mu\text{m}$  filtered Mn concentration was below the detection limit (1  $\mu\text{g/L}$ ), and the conductivity of the supernatant was sufficiently low. Particles were rinsed with deionized water but were not oven dried in order to maintain characterization similar to  $\text{MnO}_x$  present in drinking water treatment.

### **2.2.3 Mn(II) and NOM Adsorption Experiments**

Experiments were performed at room temperature ( $\sim 20$   $^{\circ}\text{C}$ ) in a Fisher Scientific<sup>TM</sup> Isotemp<sup>TM</sup> dual chamber incubator shaker for  $5 \pm 1$  hours. The requisite volume of a 0.1 M  $\text{MnSO}_4$  solution was added to 15 mL aliquots of 20 or 500 mg/L  $\text{MnO}_x$  in 15 mL Teflon centrifuge tubes.

NOM adsorption experiments were performed using 500 mg/L  $\text{MnO}_x$  in 50 mL Teflon centrifuge tubes and dissolved organic carbon (DOC) concentrations ranging from 0.5 to 30 mg/L C. Samples were allowed to equilibrate for  $24 \pm 1$  hours at  $\sim 20$   $^{\circ}\text{C}$  in the dark. The ionic strength was increased for some NOM adsorption experiments by adding 50 mM sodium chloride (NaCl) to the solutions. Twenty milligrams per liter of  $\text{Ca}^{2+}$  was used for some experiments. Other experiments combined high ionic strength with  $\text{Ca}^{2+}$

addition. Calcium chloride salt was added as the source of  $\text{Ca}^{2+}$ , and NaCl was added as the salt where pertinent.

A 5 mM carbonate buffer was used for these experiments at pH 5.1 and/or 6.1. Experiments were performed in triplicate. At the end of the reaction time samples were centrifuged at 3,500 rpm for 4 minutes, then filtered using a 30 kDa molecular weight cutoff ultra-filter (UF) in a 200-mL Amicon UF cell with stirring under nitrogen at 30 psi. Organic carbon and elemental measurements were made on the filtrate.

#### **2.2.4 DBP Formation and Kinetic Experiments**

DBP formation experiments were performed in 250 mL amber bottles at room temperature (approximately 20°C) with lateral shaking on a New Brunswick Innova 2100 platform shaker at 100 rpm. Experiments were carried out in 5 mM carbonate buffer with approximately 4 mg/L DOC and a reaction time of 6 +/- 1 hr. A stock solution of the desired  $\text{MnO}_x$  concentration (approximately 500 mg/L  $\text{MnO}_x$ ) buffered at pH 6.1 was made, NOM was added, and the solution was immediately distributed to the amber bottles. Twenty-five microliters of a 0.1 M  $\text{MnSO}_4$  solution (10  $\mu\text{M}$ ) were added to some samples to test whether adding dissolved Mn(II) affected the reaction products. Chlorine was dosed where appropriate at 3 to 5 mg/L. All experiments were performed in duplicate or triplicate. At the end of the reaction time, samples were first filtered with Millipore polycarbonate, track-etched 0.4  $\mu\text{m}$  membrane filters under vacuum to remove the  $\text{MnO}_x$  particles. Samples were then filtered with a Millipore Ultracel regenerated cellulose 30 kDa molecular weight cutoff ultra filter (UF) in a 200 mL UF cell with stirring under nitrogen at 30 psi. The dissolved (fraction that passed through the UF)

organic carbon, Mn, and DBP concentrations were measured. The chlorine residual was also measured.

Experiments with coated and uncoated media were performed similarly. Macrolite M7, a porous ceramic media with an effective size of 2 mm (characterization details provided by Bazilio et al. (2016)) was used. Approximately 20 g of coated (~ 3 mg Mn/g media) or uncoated media were added to the amber bottles, and a buffered NOM solution was added and chlorinated. The mass of media is calculated according to Equation 2.2 which shows the calculation for the mass of MnO<sub>x</sub> coated media with a coating level of 4 mg Mn/g Media needed for a MnO<sub>2</sub> concentration of 0.5 g MnO<sub>2</sub>/L (or 5.75 × 10<sup>-3</sup> M Mn) in 250 mL.

$$x \text{ g Media} = \frac{0.316 \frac{\text{g Mn}}{\text{L}}}{0.004 \frac{\text{g Mn}}{\text{g Media}}} \times 0.250 \text{ L} = 19.7 \text{ g Media} \quad \text{Equation 2.2}$$

### 2.2.5 Analysis

Manganese, calcium and magnesium were measured by inductively coupled plasma atomic emission spectroscopy (ICP-AES) or inductively coupled plasma mass spectrometry (ICP-MS). Organic carbon was measured according to standard method 5310, using a Shimadzu-TOCV Total Organic Carbon Analyzer. UV absorbance at 254 nm (UV<sub>254</sub>) measurements were made with a Genesys 10s spectrophotometer. The chlorine stock concentration was measured by the DPD titration method, and the free chlorine residual was measured by Hach method 8021 (DPD reagent).

Trihalomethanes and haloacetonitriles were determined by EPA Method 551.1 with minor modifications. Haloacetic acids were determined by EPA method 552.2 with minor modifications; a DB-1 column was used and an oven temperature program as

specified by Brophy, Weinberg and Singer (2000). Gas chromatographs (Agilent) equipped with auto samplers and electron capture detectors (GC-ECD) were used.

### **2.2.6 Particle and Media Characterization**

The MnO<sub>x</sub> concentration of the suspension was determined by first digesting the particles with hydroxylamine sulfate in 2 % (by volume) nitric acid, followed by quantification of Mn by ICP-AES. Coated granular media (Macrolite M7) MnO<sub>x</sub> coating level was determined by reductive dissolution with hydroxylamine sulfate in 2 % nitric acid, and measuring the resulting solution Mn concentration (Knocke, Ramon and Thompson (1988a)).

The surface area of the particles was determined by nitrogen adsorption BET analysis on a Quantachrome Autosorb-iQ system at 77 K after outgassing at 120 °C until pressure rise in the test cell was less than 25 mTorr/min. The MnO<sub>x</sub> surface area was 175 m<sup>2</sup>/g. Powder X-ray diffraction (XRD) patterns were collected on a PANalytical X'Pert diffractometer using Cu K $\alpha$  radiation. Data were collected in 2 $\theta$  range from 5 to 70 degrees with a step size of 0.02 degrees and a step time of 1 s. X-ray photoelectron spectroscopy (XPS) was performed on a Quantum 2000 Scanning ESCA Microprobe (Physical Electronics, Inc.) with aluminum K-alpha monochromatic x-rays and a 16 channel detector to determine Mn oxidation state. The pass energy for surveys was 187.85eV and the multiplex was 46.95 eV. Fourier transform infrared spectroscopy (FTIR) was performed on synthesized particles as well as particles after NOM adsorption experiments.

Synthesized MnO<sub>x</sub> particles were freeze dried (Labcono) and sputter coated (Hummer Anatech 6.6 system) with approximately 6 nm of gold palladium alloy for

scanning electron microscopy (SEM), or carbon for energy dispersive spectrometry (EDS). Imaging of the samples was performed using a Jeol JSM-7100F Field Emission Scanning Electron Microscope equipped with a Noran System 7 energy dispersive spectrometer.

## **2.3 Results and Discussion**

### **2.3.1 Characterization**

X-Ray diffraction of freeze dried synthesized  $\text{MnO}_x$  particles showed weak reflections at 7.9 Å and 2.4 Å, indicative of an amorphous structure. The relatively large surface area of 175  $\text{m}^2/\text{g}$  is also characteristic of the amorphous  $\delta\text{-MnO}_2$ . Characterization results confirm that the particles produced are similar to the amorphous birnessite prepared by Murray (1974).

Figure 2.1 is an SEM image of the freeze dried  $\text{MnO}_x$  particles. The  $\text{MnO}_x$  particles appear to be aggregates of smaller sub-micron particles.

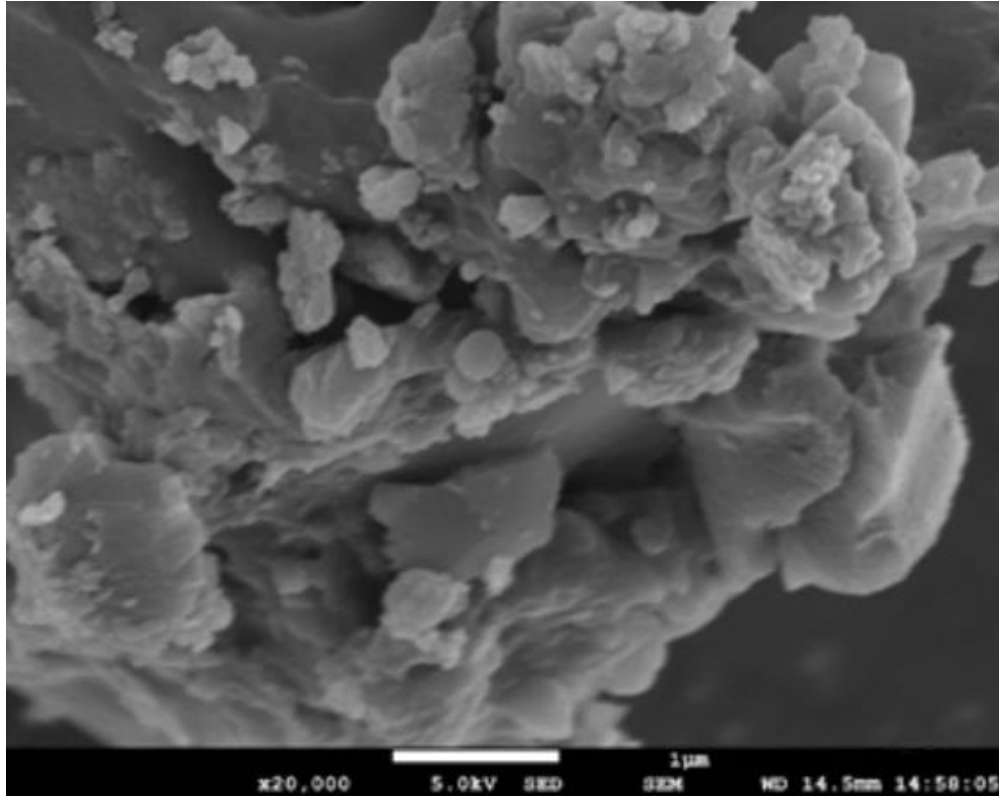


**Figure 2.1. SEM image of synthesized MnO<sub>x</sub> particles (magnification 20,000X).**

### **2.3.2 Mn(II) and NOM adsorption**

Results for Mn(II) adsorption onto the synthesized MnO<sub>x</sub> exhibited Langmuir behavior. A Langmuir adsorption isotherm fit was done using the Levenberg-Marquardt nonlinear least-squares algorithm in R and Equation 2.3:

$$q = \frac{q_{max}Kc}{1+Kc} \quad \text{Equation 2.3}$$

At pH 5.1 and 20 mg/L MnO<sub>x</sub> (Figure 2.2), a maximum adsorption density ( $q_{max}$ ) of 115 mg Mn/g MnO<sub>x</sub> and an adsorption constant ( $K$ ) of 108 L/mg were obtained. These results confirm that the synthesized MnO<sub>x</sub> adsorbs Mn(II) at relatively low pH and low MnO<sub>x</sub> concentrations. At pH 6.1 with 300 mg/L MnO<sub>x</sub>,  $q_{max}$  was 87.2 mg Mn/g MnO<sub>x</sub> and  $K$  was 410 L/mg.

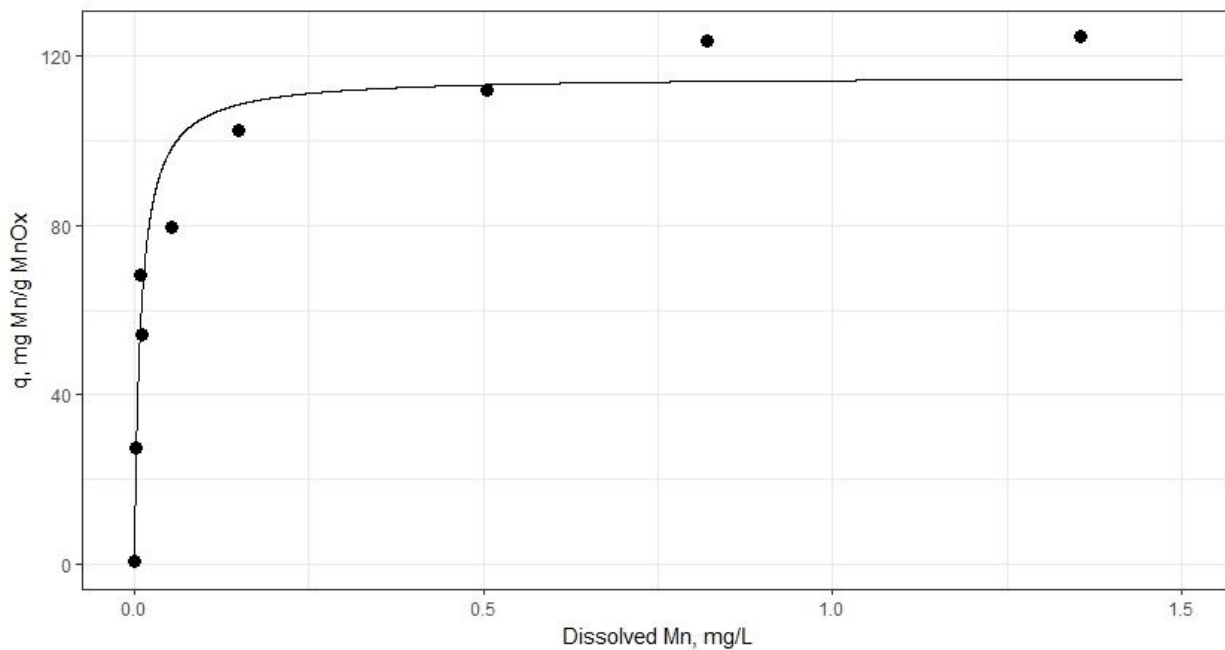


**Figure 2.2. Mn(II) adsorption isotherm and modeled Langmuir fit at pH 5.1 using a 20 mg/L MnO<sub>x</sub> suspension at room temperature.**

The affinity of divalent cations for MnO<sub>x</sub> surfaces decreases in the order Mg<sup>2+</sup> < Ca<sup>2+</sup> < Zn<sup>2+</sup> < Mn<sup>2+</sup>. While the MnO<sub>x</sub> Zn<sup>2+</sup> adsorption capacity was a little lower than that of Mn<sup>2+</sup>, the Ca<sup>2+</sup> and Mg<sup>2+</sup> adsorption capacities were consistently less than half of the Mn<sup>2+</sup> capacity from pH 2 to 7.5 (Murray (1975); Morgan and Stumm (1964)).

NOM adsorption results showed no measurable adsorption for experiments performed using DOC concentrations of 0.25 to 12 mg/L DOC and MnO<sub>x</sub> concentrations as high as ~0.5 g/L and pH ranging from 5 to 7. The DOC fraction of aquatic, water soluble, humic substances is generally made up of low to moderate molecular weight anionic polyelectrolytes. Aquatic DOC is complex and consists of carboxylic and

phenolic groups. The carboxylic groups are deprotonated at pH greater than 2 (Thurman (1985)).

In the pH range of the adsorption experiments, the  $\text{MnO}_x$  surface and the NOM were negatively charged resulting in electrostatic repulsion, one reason for no measurable NOM adsorption. NOM adsorption involves the adsorption of a mixture of adsorbates as well as adsorption of a polymeric species. Aquatic humic substance (HS) adsorption increases with decreasing pH, specifically pH below the oxide  $\text{pH}(\text{ZPC})$ ; the  $\text{pH}(\text{ZPC})$  of the synthesized  $\text{MnO}_x$  particles is assumed to be less than  $\sim 2.5$  as measured by Murray (1974). Tipping and Heaton (1983) showed that HS adsorption to two different oxides of Mn increased by increasing divalent cation concentration ( $\text{Ca}^{2+}$  was used). The purported mechanism was by either acting as a bridge between the negatively charged oxide surface groups and the NOM, or by decreasing the electrostatic repulsion between the groups. Liu et al. (2009) proposed that  $\text{Ca}^{2+}$  ions can facilitate  $\delta\text{MnO}_2$  aggregation in addition to coordination with surface hydroxyls, and as a result enhance humic acid adsorption by the  $\delta\text{MnO}_2$ .

Calcium ion addition (20 mg/L or 0.5 mM  $\text{Ca}^{2+}$ ) increased the adsorption density of NOM to the  $\text{MnO}_x$  particles for a  $q_{max}$  of approximately 3 mg OC/g  $\text{MnO}_x$  at pH 6.1. Increasing the ionic strength by adding 50 mM of NaCl resulted in a  $q_{max}$  of approximately 3 mg OC/g  $\text{MnO}_x$ . The highest adsorption density resulted in experiments with both NaCl and  $\text{Ca}^{2+}$  present;  $q$  was approximately 10 mg OC/g  $\text{MnO}_x$  (Figure 2.3).

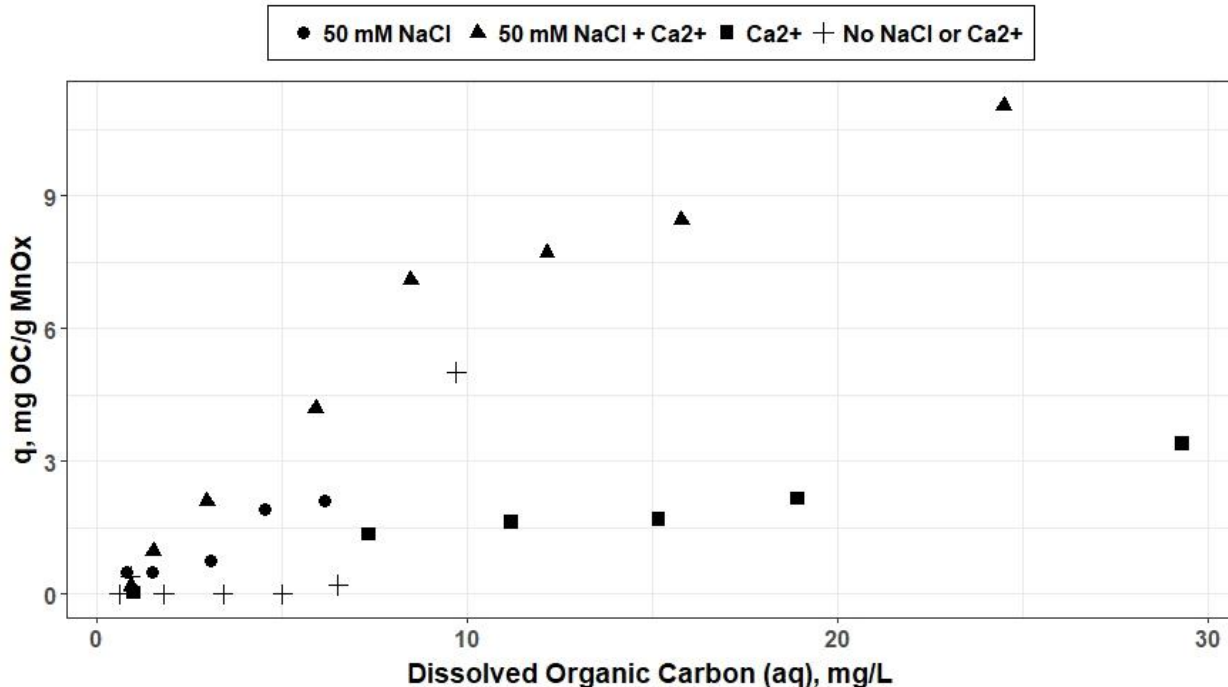


Figure 2.3. NOM adsorption isotherms for different ionic strengths and Ca<sup>2+</sup> concentrations. pH 6.1 using a 0.5 g/L MnO<sub>x</sub> suspension at ~20 °C for 24 ± 1 hours; 5mM carbonate buffer, 0.5 mM Ca<sup>2+</sup>.

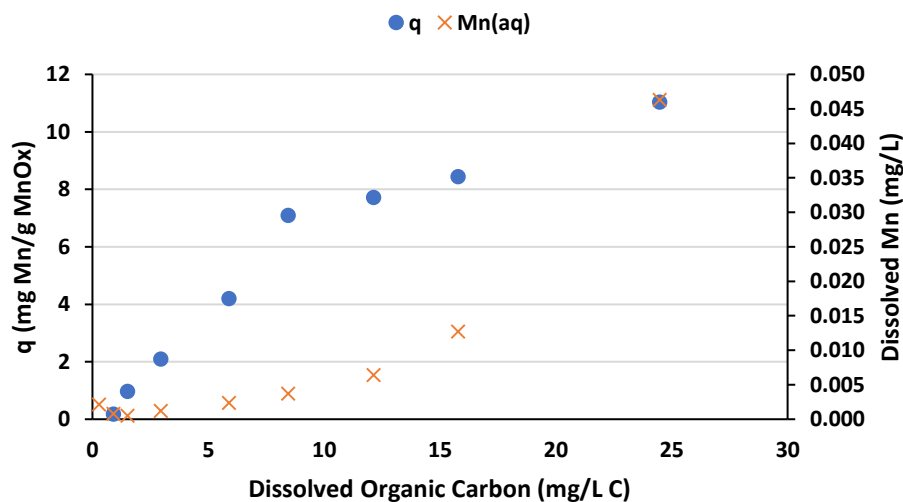
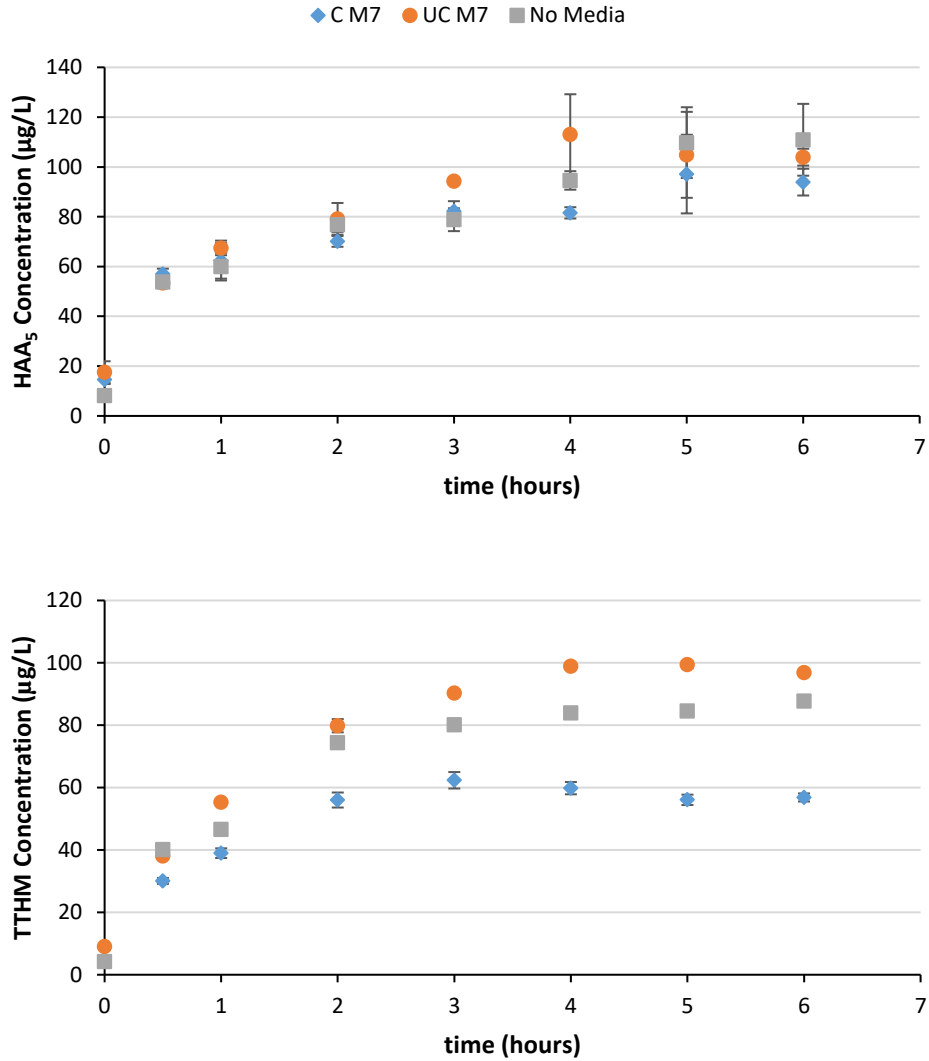


Figure 2.4. Change in dissolved organic carbon concentration and Mn(II) evolution at high ionic strength (50 mM NaCl) in the presence of Ca<sup>2+</sup> ions (0.5 mM) and 0.5 g/L MnO<sub>x</sub>.

Figure 2.4 shows adsorbed organic carbon and dissolved Mn concentrations after 24 hours. The increase in dissolved Mn suggests that the  $\text{MnO}_x$  was reduced, and that the DOC was oxidized. Gallard et al. (2009) proposed that  $\text{MnO}_x$  oxidizes NOM, and Wang and Stone (2006a) showed that birnessite oxidized organic compounds with functional groups similar to those found in aquatic NOM.

### **2.3.3 DBP Formation**

Disinfection byproduct formation was examined in batch experiments with coated (C M7) and uncoated (UC M7) granular Macrolite media, and with synthesized  $\text{MnO}_x$  particles. Figure 2.5 shows that  $\text{HAA}_5$  and TTHM concentrations increased with increased reaction times using 4 mg/L DOC at pH 6.9 and room temperature with a chlorine residual of approximately 1 mg/L. The  $\text{HAA}_5$  concentrations were approximately the same when there was no media, coated media, or uncoated media. The TTHM concentrations for uncoated media were approximately 9  $\mu\text{g/L}$  higher than TTHM concentrations with no media present for reactions time greater than 2 hours. The TTHM concentrations for samples with coated media present decreased slightly after 3 hours, and were 18  $\mu\text{g/L}$  to 30  $\mu\text{g/L}$  lower than TTHM concentrations for samples with no media present.



**Figure 2.5 (a) HAA<sub>5</sub> and (b) TTHM concentrations over time using ~4 mg/L DOC, residual Cl<sub>2</sub> ~ 1mg/L after 6 hours, and coated or uncoated granular media at pH 6.9 ± 0.2.**

Figure 2.6 shows that HAA<sub>5</sub> concentrations increase with increasing DOC concentrations after 4 hours in the presence or absence of MnO<sub>x</sub> at pH 6.1 with approximately 1 mg/L residual Cl<sub>2</sub>. Equal concentrations resulted for samples with no MnO<sub>x</sub> or MnO<sub>x</sub> for concentrations of DOC less than 3 mg/L. At a DOC concentration of

4 mg/L, the average HAA<sub>5</sub> concentration was 8 µg/L greater in samples with MnO<sub>x</sub> than in samples without particles.

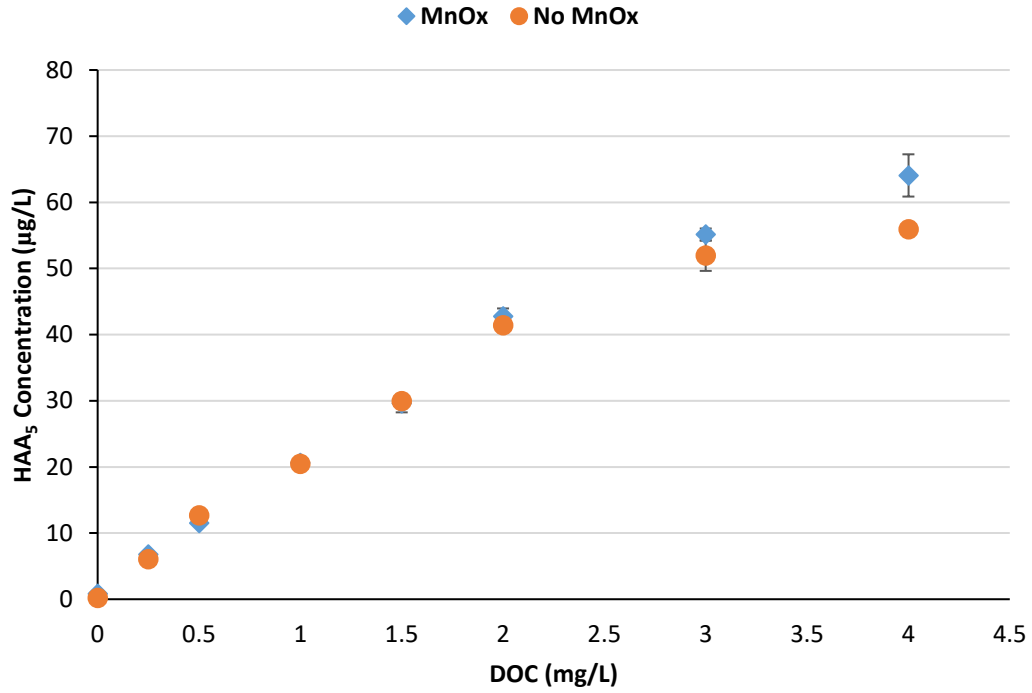


**Figure 2.6. HAA<sub>5</sub> formation for different initial DOC concentrations after 4 hours at pH 6.1 ± 0.2, residual Cl<sub>2</sub> ~ 1mg/L, with 0.5 g/L MnO<sub>x</sub> or no MnO<sub>x</sub>.**

Figure 2.7 shows the concentrations of HAA<sub>5</sub> and TTHMs formed with no media present, uncoated media (UC M7), and coated media (C M7), with and without dissolved manganese (Mn(II)) at pH 6. Generally, HAA<sub>5</sub> concentrations were 18% to 28% higher when there was media (a surface) present. A MnO<sub>x</sub> coating on the media did not result in a measurable difference as compared to having uncoated media present in experiments without Mn(II). TTHM concentration was slightly higher when uncoated media was present and lower when MnO<sub>x</sub> coated media was present as compared to reactions with no media. Chloroform accounted for more than 99% of the TTHMs formed. HAA<sub>5</sub> and

TTHMs concentration ranges for no-, coated- and uncoated- media generally overlapped indicating no measured difference in formation.

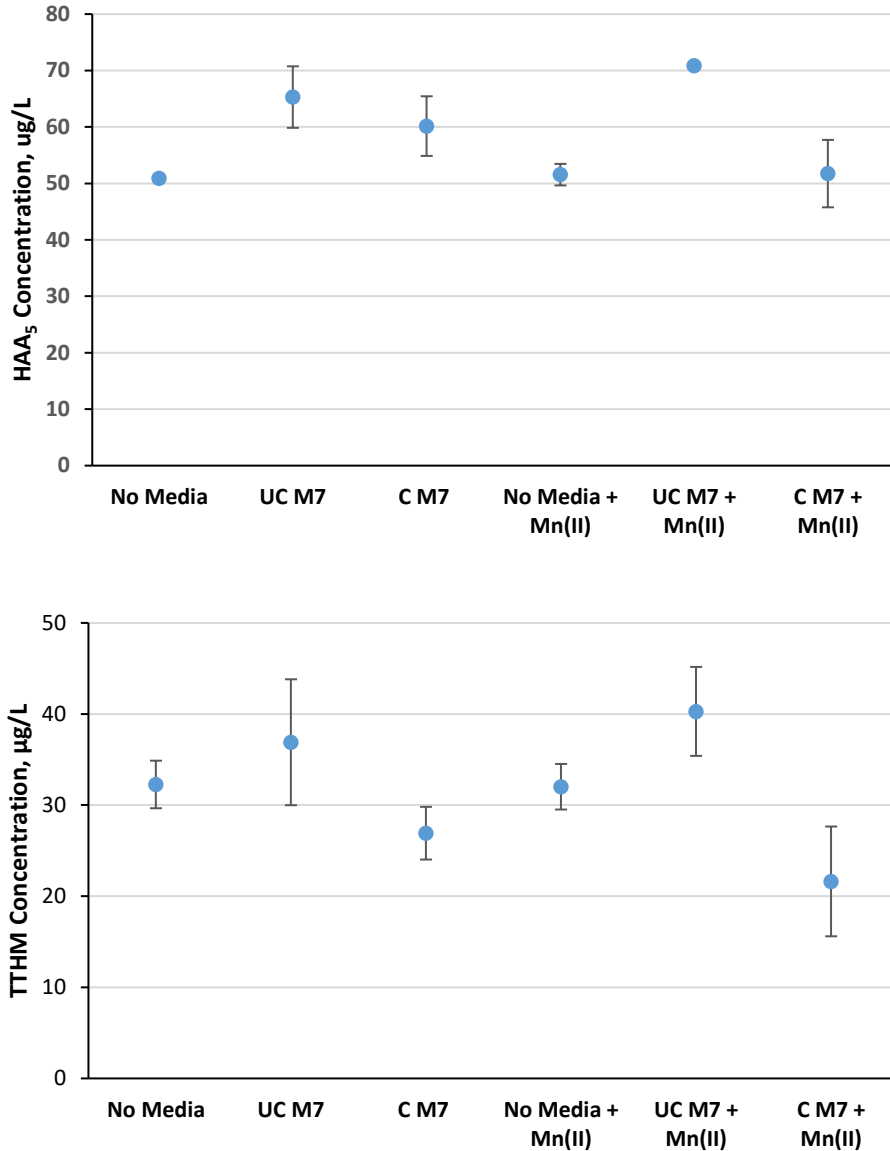


**Figure 2.7. (a) HAA<sub>5</sub> and (b) TTHM concentrations formed when NOM was chlorinated with no media, uncoated or coated media present. Reaction time 5 hours, residual Cl<sub>2</sub> ~0.5 mg/L, ~ 4 mg/L DOC, UV<sub>254</sub> 0.14 cm<sup>-1</sup>, where present 0.55 mg/L Mn(II), at pH 6.0 ± 0.2.**

In experiments with no surface present, introducing Mn(II) at the beginning of the reaction did not impact the DBP concentrations (51  $\mu\text{g/L}$  compared to 52  $\mu\text{g/L}$  HAA<sub>5</sub>; 32  $\mu\text{g/L}$  TTHM in both cases). Of note is the difference between HAA<sub>5</sub> concentrations for samples with uncoated media versus coated media when Mn(II) was present at the beginning of the reaction. The TTHM and HAA<sub>5</sub> concentrations were approximately 18  $\mu\text{g/L}$  greater in samples with uncoated media compared to those of samples with no media, while the average TTHM and HAA<sub>5</sub> concentrations of samples with coated media were similar to samples with no media.

Adsorption of the Mn(II) to the MnO<sub>x</sub> coating on the coated media, and subsequent oxidation by the chlorine could explain the lower DBP concentrations. The homogeneous reaction between chlorine and Mn(II) is much slower than that between chlorine and NOM. As a result, more DBPs could have formed during the reaction because the chlorine-Mn(II) reaction was not exerting a chlorine demand. In the samples with MnO<sub>x</sub> coated media, the oxidation of the sorbed Mn(II) exerted a chlorine demand, and the reaction kinetics (closer to those of the NOM-chlorine reaction) allowed for competing parallel reactions.

Table 2.1 shows resulting HAA<sub>5</sub>, DCAA, TCAA, and TTHM concentrations using MnO<sub>x</sub> particles when NOM was chlorinated in the presence and absence of Mn(II). The average concentrations of the HAAs were marginally higher in chlorinated samples with Mn(II) present, a difference of 3  $\mu\text{g/L}$  in HAA<sub>5</sub> concentration. TTHM concentrations were the same with and without Mn(II) present.

More than 99% of dissolved Mn added to samples with initial Mn(II) (0.55 mg/L) was adsorbed by the MnO<sub>x</sub> by the end of the reaction period. In samples with Mn(II) and

MnO<sub>x</sub> but no chlorine, the Mn(II) was removed by adsorption to the original MnO<sub>x</sub> only.

Where present, chlorine oxidized the adsorbed Mn(II), regenerating the MnO<sub>x</sub>.

**Table 2.1. HAA<sub>5</sub> and TTHM concentrations using ~ 0.5 g/L MnO<sub>x</sub> particles in presence or absence of Cl<sub>2</sub> and/or Mn(II). Reaction time 5 hours, residual Cl<sub>2</sub> ~1 mg/L, ~ 4 mg/L DOC, where present 0.55 mg/L Mn(II), at pH 6.1 ± 0.2.**

	Concentration (µg/L)				Mn(II) (mg/L)
	HAA <sub>5</sub>	DCAA	TCAA	TTHM	
NOM + MnO <sub>x</sub>	0.1 ± 0.1	0.07 ± 0.02	0.05 ± 0.05	1.2 ± 0.2	0.002
NOM + MnO <sub>x</sub> + Mn(II)	0.2 ± 0.1	0.08 ± 0.03	0.1 ± 0.1	1.0 ± 0.2	0.001
NOM + MnO <sub>x</sub> + Cl <sub>2</sub>	18.0 ± 1.4	13.0 ± 0.8	4.9 ± 0.6	5.4 ± 1.0	0.001
NOM + MnO <sub>x</sub> + Mn(II) + Cl <sub>2</sub>	21.0 ± 1.5	14.9 ± 0.8	6.1 ± 0.7	5.5 ± 0.7	0.002

#### 2.3.4 Kinetic Studies

Kinetic experiments were performed at 20 °C with 0.5 g/L of MnO<sub>x</sub> particles at pH 6.3 ± 0.2 using a chlorine dose of 5 mg/L, approximately 3.5 mg/L DOC, and 0.55 mg/L Mn(II) when added. Both dichloroacetic acid (DCAA) and trichloroacetic acid (TCAA) formed rapidly upon chlorination, increasing exponentially within the first few minutes then linearly over time when chlorine was present in excess (Figure 2.8).

An examination of the linear region showed that the reaction rates for DCAA and TCAA formation were marginally greater with Mn(II) present (Figure 2.9), although the final TCAA and DCAA concentrations did not greatly differ.

In the pH range of 5 to 7, the δMnO<sub>x</sub> surface sites and the NOM are assumed to be negatively charged. The higher HAA concentrations when Mn(II) is introduced at the beginning of the reaction may be the result of a similar phenomenon observed by Wang and Stone (2006a) where Mn(II) formed complexes with the negatively charged citrate, and these complexes attached more readily to surface Mn<sup>III,IV</sup>. The attachment to and/or

transformation of the NOM by the  $MnO_x$  may lower the activation energy for the NOM- $HOCl$  reaction resulting in the marginally higher reaction rate.

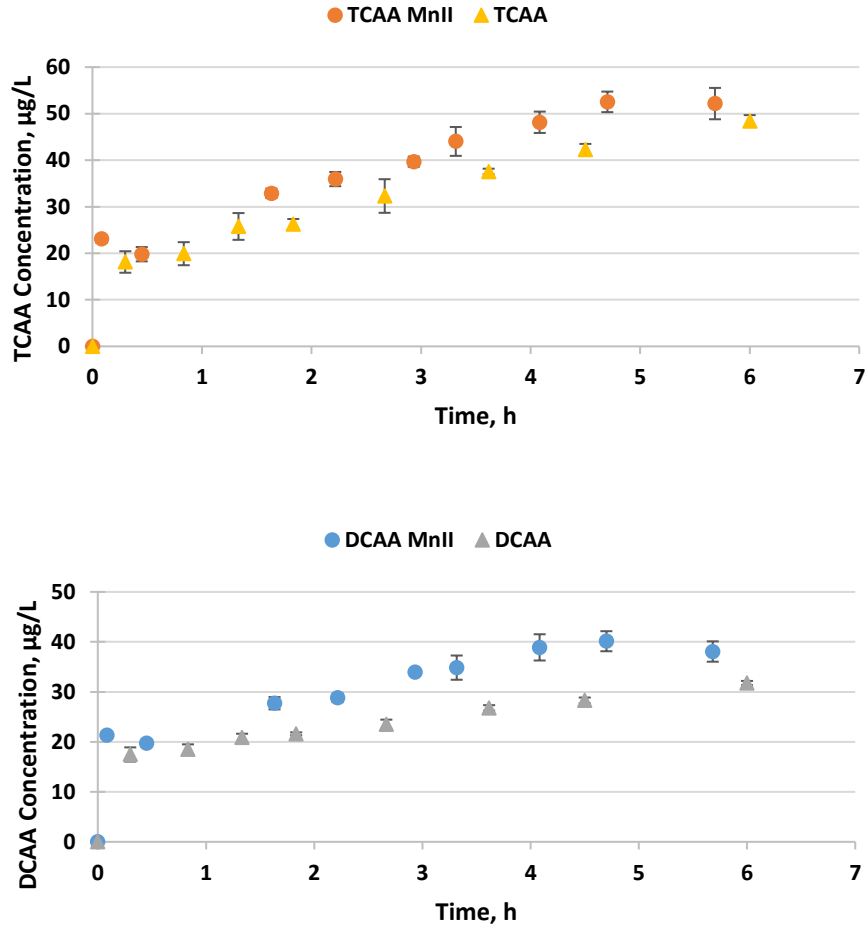


**Figure 2.8. (a) TCAA and (b) DCAA concentrations over time with and without 0.55 mg/L Mn(II). Approximately 0.5 g/L  $MnO_x$ , ~3.5 mg/L DOC, pH  $6.3 \pm 0.2$ , ~2 mg/L residual  $Cl_2$ .**

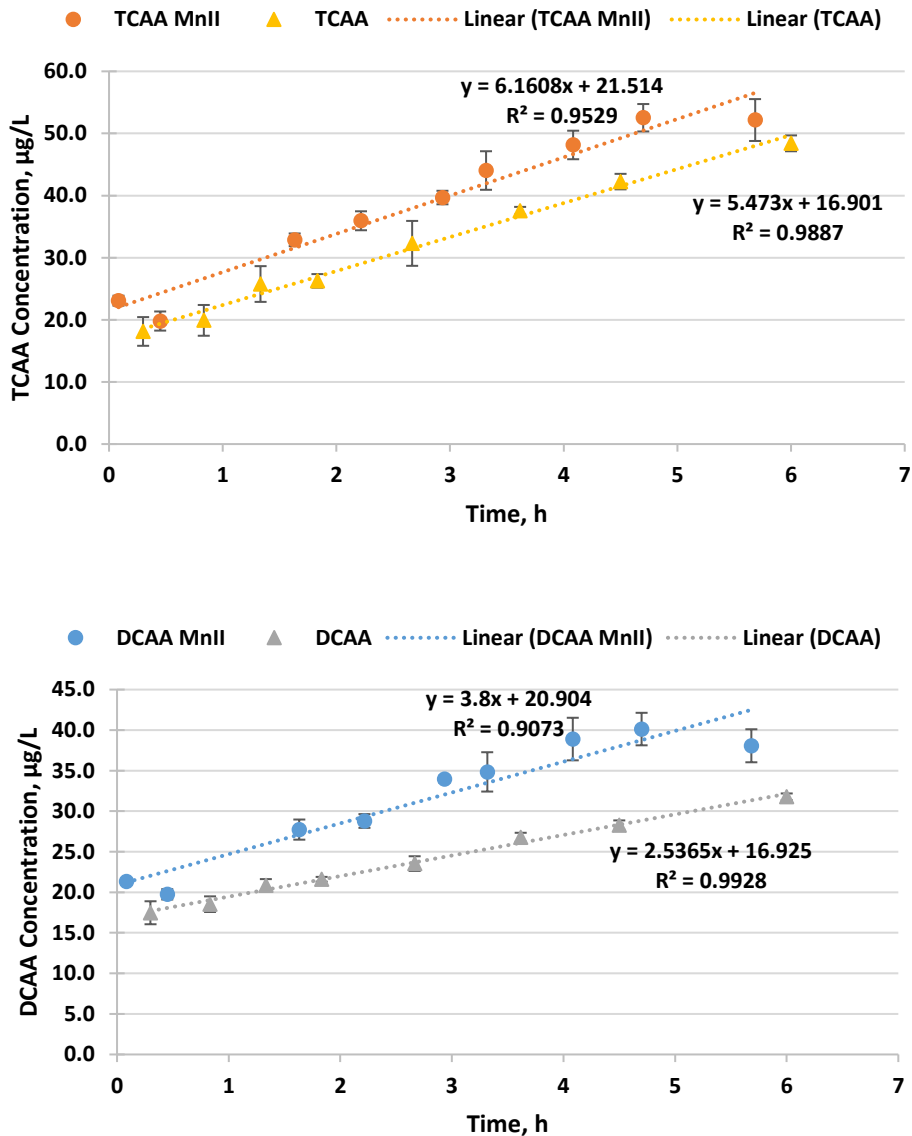


**Figure 2.9. Linear region of (a) TCAA and (b) DCAA formation.**

Clarified water (sedimentation basin effluent prior to chlorination) from a nearby utility was used to perform DBP formation kinetic studies under conditions conducive to NOM attachment. The water contained 18 mg/L Ca and 3 mg/L Mg, and 0.30 mg/L Mn(II). The water was dosed with 6 mg/L Cl<sub>2</sub> in the presence and absence of MnO<sub>x</sub> particles.

The pH of the water was 6.5, and the pH was not controlled for these samples. The DOC (2.1 mg C/L) of the water remained unchanged in all reactions. When no MnO<sub>x</sub> was present, the UV<sub>254</sub> absorbance remained mostly unchanged, and showed the greatest decrease from 0.045 to 0.037 after 5 hours; the dissolved Mn concentration decreased from 0.30 to 0.11 mg/L on average for all of the samples. In the samples with 0.5 g/L MnO<sub>x</sub> particles, the UV<sub>254</sub> absorbance was 0.033 after 5 hours, and the dissolved Mn concentration decreased from 0.30 mg/L to 0.03 mg/L on average for all samples.

Figure 2.10 shows the DBP concentrations over time formed upon chlorinating the clarified water. Dibromochloromethane (DBCM), one of the four TTHMs, concentrations are presented because of a temporary failure in chloroform measurement. HAA<sub>5</sub> concentrations were approximately 10% greater over time in samples with no MnO<sub>x</sub> than in samples with MnO<sub>x</sub>. BDCM concentrations were 33% greater in samples without MnO<sub>x</sub> than in samples with MnO<sub>x</sub>.

The chlorine residual in samples without MnO<sub>x</sub> ranged from 3.7 mg/L Cl<sub>2</sub> for the close to instantaneous reaction time (2.5 minutes) to 2.3 for the longest reaction time (5 hours). In samples with MnO<sub>x</sub> the chlorine residual ranged from 3.5 mg/L Cl<sub>2</sub> for the close to instantaneous reaction time (3 minutes) to 0.5 mg/L Cl<sub>2</sub> for the longest reaction time (5 hours). The catalytic oxidation of Mn(II) exerted a chlorine demand of 0.39 mg/L Cl<sub>2</sub>, resulting in the lower chlorine residuals after 5 hours in the samples with MnO<sub>x</sub>.

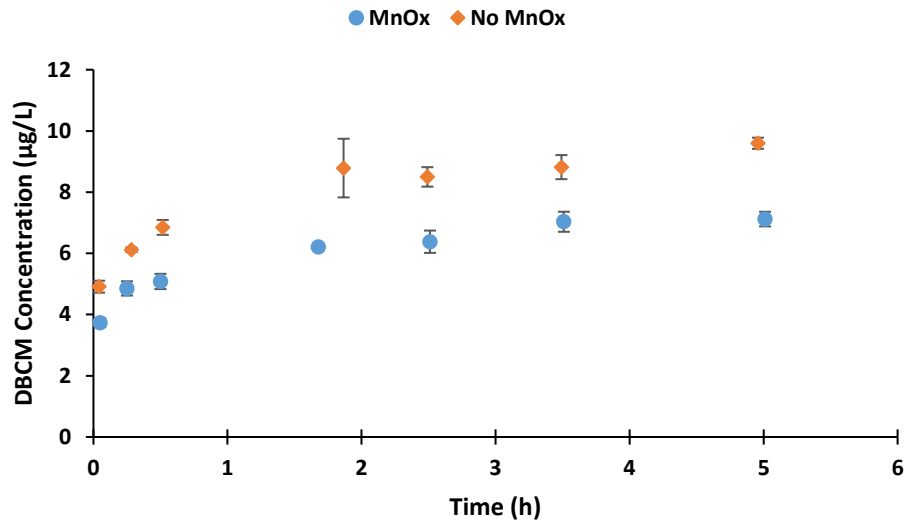
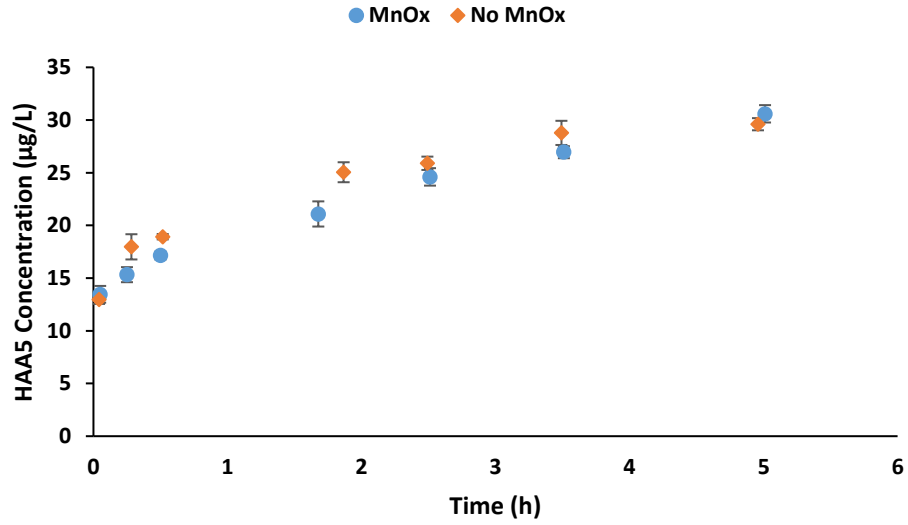


**Figure 2.10. HAA<sub>5</sub> and DBCM concentrations overtime using a clarified surface water. MnO<sub>x</sub> concentration 0.5 g/L, pH 6.5, [Mn(II)] = 0.30 mg/L, DOC = 2.1 mg C/L.**

The higher chlorine residual may explain why the DBP concentrations of samples were 3% to 35% greater in samples without MnO<sub>x</sub>.

## 2.4 Conclusions

While Mn(II) readily adsorbed to MnO<sub>x</sub> particles and MnO<sub>x</sub> coated surfaces under conditions similar to those found in drinking water treatment, NOM did not. The MnO<sub>x</sub> therefore is not likely to adsorb or oxidize DOC in typical plants practicing Mn(II) removal by sorption to MnO<sub>x</sub> coated granular media and catalytic oxidation by free chlorine.

The presence of MnO<sub>x</sub> or MnO<sub>x</sub> coated surfaces does not appear to increase DBP formation due to the reactions between NOM and free chlorine. For water treatment plants applying pre-filter chlorine for Mn(II) catalytic oxidation across MnO<sub>x</sub>-coated granular media this means that resulting increases in filter effluent DBP concentrations as compared to application of free chlorine after media filtration are mainly functions of media associated NOM (along with time, pH, temperature etc.), not the MnO<sub>x</sub> surfaces. If DBP concentrations are unacceptably high and pre-filter chlorination is undesirable, an alternative method for Mn(II) removal should be considered.

## CHAPTER 3

### IMPACT OF MANGANESE OXIDE-COATED GRANULAR FILTER MEDIA ON DISINFECTION BYPRODUCT FORMATION

#### 3.1 Introduction

Dissolved manganese (Mn(II)) in source water can generally be removed by oxidation by a strong oxidant (such as permanganate, chlorine dioxide or ozone) to form insoluble MnIII/IV oxides ahead of particle removal, or by sorption to manganese oxide (MnO<sub>x</sub>) coated granular filter media followed by catalytic oxidation by free chlorine. Microbially mediated Mn(II) oxidation to Mn(IV) by media-associated microorganisms is also an important removal process. The selection of the removal process is dependent on Mn concentration and form, as well as other source water parameters such as pH, alkalinity, iron, natural organic matter (NOM), and other constituents. For waters with considerable amounts of dissolved iron (Fe(II)) or organic carbon which exert an oxidant demand or for water with seasonally elevated Mn(II), strong oxidants may be less effective for Mn(II) oxidation (Tobiason et al. (2016)).

The catalytic oxidation of sorbed Mn(II) by free chlorine is rapid at pH > 6, and available Mn(II) adsorption sites are regenerated as more MnO<sub>x</sub> is formed. In the absence of free chlorine Mn(II) removal occurs by adsorption only. Mn(II) adsorption to MnO<sub>x</sub> is promoted by alkaline conditions. If reducing conditions develop, Mn(II) may be released from MnO<sub>x</sub>-coated filter media (Knocke, Occiano and Hungate (1991); Knocke, Ramon and Thompson (1988b)).

Disinfection byproducts (DBPs) which may be formed during disinfection are known to be genotoxic and carcinogenic (Richardson (2003)), and some DBPs are regulated by the U.S Environmental Protection Agency (EPA). The total trihalomethanes (TTHMs) and five haloacetic acids (HAA<sub>5</sub>) are two groups of halogenated organics with maximum contaminant limits (MCLs) on a locational running annual average basis of 80 µg/L and 60 µg/L respectively.

Corbin et al. (2003) showed that pre-filter chlorination resulted in higher DBP concentrations in more than 80% of simulated distribution samples as compared to DBP levels for post-filter chlorination only. However, pre-filter chlorination is needed as discontinuation may result in Mn(II) release from MnO<sub>x</sub>-coated media and pre-filter chlorine is needed to remove seasonally elevated Mn(II). Otherwise, an alternative method for Mn(II) removal would be needed. The results of bench- and full-scale experiments examining DBP formation across anthracite/sand filters suggested that accumulated particulate NOM on filter media reacted with chlorine to produce DBPs (Brown (2006)). The possible role of the media MnO<sub>x</sub>-coating in increasing DBP formation was not determined.

Korshin, Benjamin and Sletten (1997) found that aromatic and carboxylic carbon-rich acidic fractions of NOM preferentially adsorbed to iron-oxide-coated sand (IOCS). Fewer studies have examined the adsorption of aquatic NOM to manganese oxides (Tipping and Heaton (1983); Gallard et al. (2009)) than to iron and aluminum oxides (Tipping (1986); Korshin, Benjamin and Sletten (1997); Gu et al. (1994); Tipping (1981); Tipping and Cooke (1982); Weng et al. (2006); Day et al. (1994); Davis and Gloor (1981)). NOM adsorption to iron oxides generally increases as pH decreases below 7, and

iron oxides are typically positively charged at  $\text{pH} < 8$  (Korshin, Benjamin and Sletten (1997)). However, amorphous manganese oxides (typically formed during sorption and catalytic oxidation in a WTP) have a lower pH of zero point of charge ( $\text{pH}(\text{ZPC})$ ), e.g.,  $\text{pH}(\text{ZPC}) \leq 5$  (Healy, Herring and Fuerstenau (1966)).

Using spectroscopic and thermogravimetric methods, Johnson et al. (2015) proposed that dissolved organic carbon (DOC) was strongly adsorbed by carboxylate functional groups to the birnessite on oxide-coated sand obtained from a drinking water treatment plant (WTP). The authors postulated that the “carboxylate groups are involved in bridging and/or bidentate bonds that bind DOC molecules to birnessite both at the mineral surface and within the bulk mineral.” They also proposed that these bonds combined with “the physical trapping of DOC within the ‘onion shell’ layers of the birnessite coating” resulted in two main organic carbon fractions associated with  $\text{MnO}_x$  coatings. The authors further speculated that polymerization reactions may occur within the mineral layers. However, the study only examined 40 year-old oxide-coated media from one WTP; historic water quality parameters were not provided as they were not within the scope of the study. Nevertheless, the results showed that organic carbon can be incorporated into the  $\text{MnO}_x$  coating on WTP filter media over time in some systems under certain conditions.

The objectives of this study were to determine the impact of  $\text{MnO}_x$ -coated granular filter media on DBP formation for  $\text{Mn}(\text{II})$  and NOM concentrations typical of drinking water treatment. Laboratory column experiments were performed using coated and uncoated anthracite, with pre- or post- column chlorination. Tests were also

performed at the full scale to determine the impact of  $\text{MnO}_x$ -coated filter media on DBP formation.

## **3.2 Materials and Methods**

### **3.2.1 Column Experiments**

#### **3.2.1.1 Column Setup**

Columns 24.1 cm (9.5 in) long with 4.21 cm (1.66 in) internal diameter and a volume of  $336 \text{ cm}^3$  ( $10.3 \text{ in}^3$ ) were used. Column media depths were approximately 6 in. The hydraulic loading rate (HLR) was  $4 \text{ gpm/ft}^2$  corresponding to a flow of  $230 \text{ mL/min}$  and an empty bed contact time (EBCT) of  $\sim 1.2$  minutes. Chlorine was dosed to achieve column effluent residuals of  $0.5$  to  $1 \text{ mg/L}$  to ensure  $\text{MnO}_x$  regeneration.

Figure 3.1 shows a schematic of the column setup. Water was pumped at a flow of  $230 \text{ mL/min}$  from a feed tank using a Cole Parmer gear pump, and chlorine was dosed inline using a Cole Parmer 7553-70 peristaltic pump at a flow rate of approximately  $6 \text{ mL/min}$  (chlorine stock concentration  $\sim 60 \text{ mg/L}$ ). Prior to experiment runs, the exact influent chlorine dose was measured for the flow rate being used.

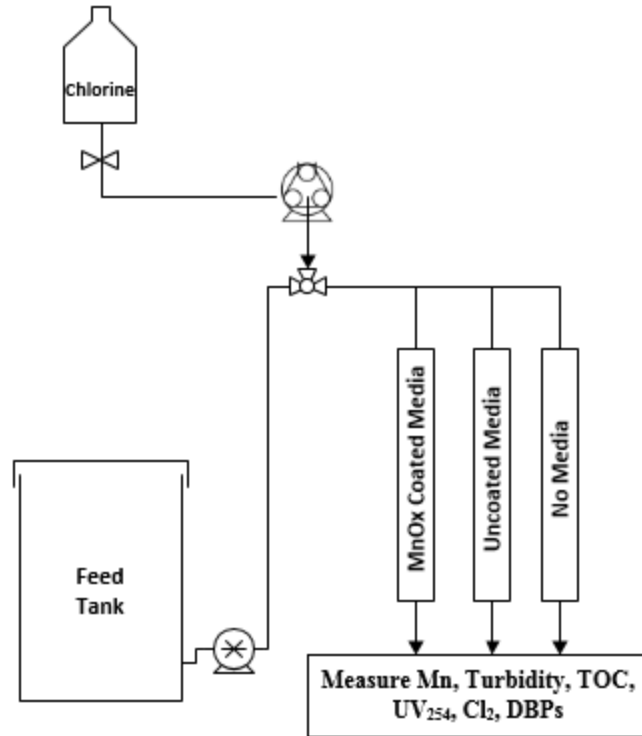


**Figure 3.1. Schematic of column setup.**

Column runs were performed with pre-column chlorination, through columns containing either uncoated anthracite, MnO<sub>x</sub> coated anthracite, or no granular media. Deionized water (DI) was first run through the columns to determine whether media-associated organic matter contributed to DBP formation. Settled water from a nearby surface water treatment plant was then pumped through the columns and samples were collected at different time intervals. Samples for instantaneous DBP measurements were immediately quenched and stored at 4 °C until they were extracted. Additional samples were collected headspace free in 300 mL biochemical oxygen demand (BOD) bottles and kept in the dark at room temperature for 24 hours. After 24 hours, aliquots were quenched for DBP analysis, and the chlorine residual was measured.

### 3.2.1.2 Granular Media

Anthracite was used as it is commonly used in granular media filters in conventional treatment plants aiming to achieve Mn(II) removal across the media filters. Uncoated anthracite from an active filter at a surface water treatment plant with low source water Mn(II) that is not practicing pre-filter chlorination (Stonington, CT) was also used. The MnO<sub>x</sub>-coated anthracite used in the column experiments was from a plant employing pre-filter chlorination ahead of MnO<sub>x</sub> coated anthracite and sand media for Mn(II) removal (Shelton, CT). Media oxide coatings of the anthracite used in experiments were determined by extraction with hydroxylamine sulfate in 2 % (by volume) nitric acid and elemental analysis by inductively coupled plasma mass spectrometry (ICP-MS) after Knocke, Occiano and Hungate (1990).

### 3.2.1.3 Column Influent

Settled water from the Putnam WTP (Greenwich CT) was collected and used in experiments. The 20 mgd capacity surface water treatment plant experiences seasonally high Mn(II) and algae; Table 3.1 summarizes the raw water quality from 2014 to 2016.

**Table 3.1. Summary of Putnam WTP raw water quality from January 2014 to December 2016.**

	pH	Total Alkalinity (mg/L CaCO <sub>3</sub> )	Turbidity (NTU)	Total Mn (mg/L)	UV <sub>254</sub> (cm <sup>-1</sup> )	TOC	DOC	Algae (total SU/mL)
Average	7.23	44	1.97	0.21	0.103	3.37	3.13	768
Maximum	8.2	62	4.6	1.29	0.161	6.02	5.95	1328
Minimum	6.58	27	0.8	0.02	0.055	2.23	1.93	61

A schematic of the treatment system is included in Figure 3.2. Chlorine dioxide (ClO<sub>2</sub>) use as a pre-oxidant began in 2013 when the plant began experiencing decreased

filter runtimes. The ClO<sub>2</sub> was typically turned on in June for about 6 months; in 2014 free chlorine was used as the pre-oxidant for a month because the ClO<sub>2</sub> generation system was not online. The ClO<sub>2</sub> dose was increased from 2014 to 2016 to control filter runtime. Chlorite is a byproduct of ClO<sub>2</sub> disinfection and has an MCL of 1.0 mg/L. Table 3.2 summarizes key water quality parameters at the time of water collection; ClO<sub>2</sub> was in use.

**Table 3.2. Water quality parameters at the time of collection of Putnam settled water.**

	pH	UV <sub>254</sub> (cm <sup>-1</sup> )	TOC (mg/L)	DOC (mg/L)	Mn Concentration (mg/L)		
					Particulate	Colloidal	Dissolved
Raw Water	6.99	0.144	5.2	5.2	0.05	0	0.40
Sedimentation Effluent	6.55	0.039	3.1	2.7	0	0.01	0.30
Filter Influent	6.55	0.048	3.0	2.7	0	0.01	0.17
Filter Effluent	6.87	0.033	2.9	2.5	0	0	0.03
Plant Effluent	7.39	0.032	2.6	2.7	0	0	0.02

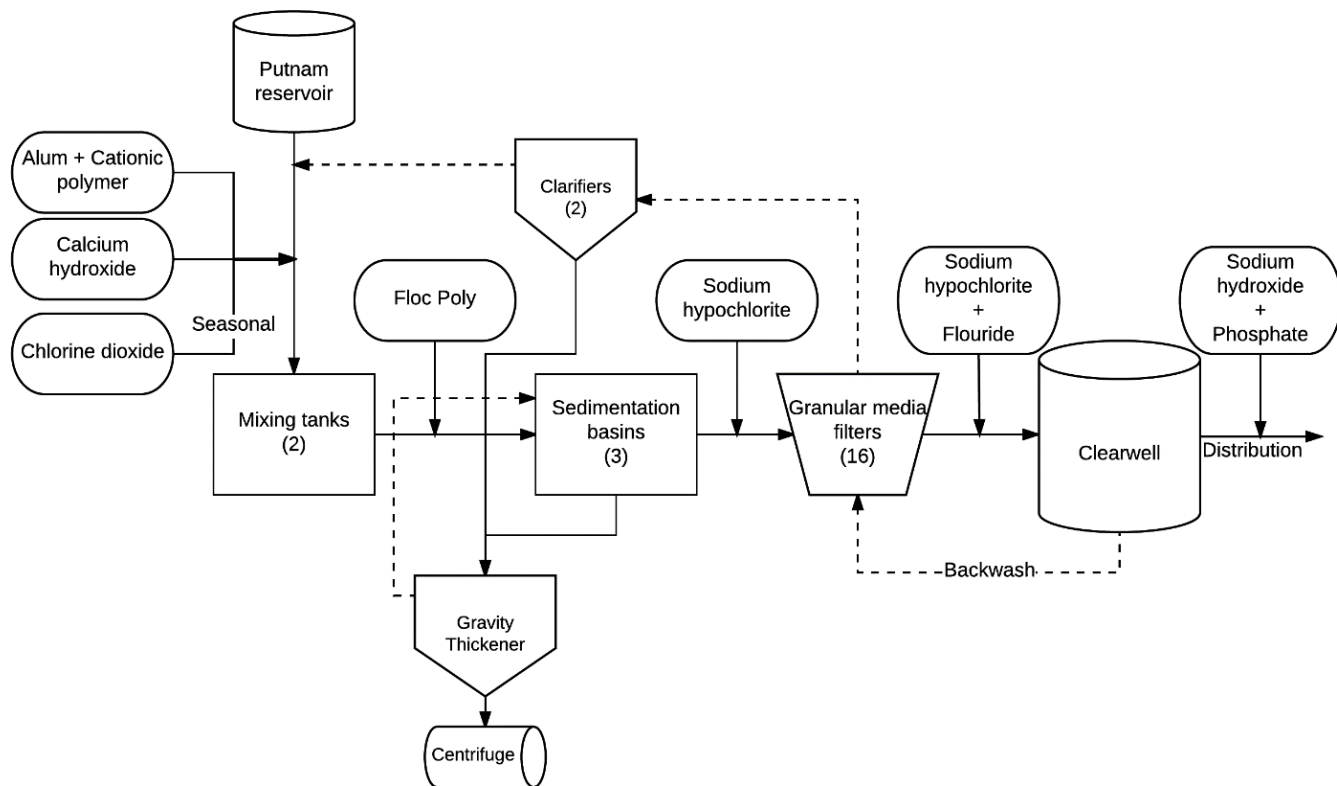


**Figure 3.2. Schematic of Putnam WTP (adapted from 2017 Putnam Report).**

### 3.2.2 Full Scale Experiments

At various times between May 2014 and June 2017, filter influent and effluent samples were collected from the Putnam WTP and held for 24 hours. DBP concentrations were then measured to determine whether contact with a  $MnO_x$  coated surface increased DBP formation. Between April 2014 and September 2015, influent and effluent samples of the second stage contactors (SSCs) at the Lantern Hill WTP (plant details in Chapter 4) were similarly held and analyzed for DBPs.

### **3.2.3 Analysis**

Trihalomethanes and haloacetic acids were determined by EPA Methods 551.1 and 552.2, respectively, with minor modifications. A DB-1 column was used for HAA analysis and an oven temperature program as specified by Brophy, Weinberg and Singer (2000). Agilent Technologies 6890 Network gas chromatographs equipped with auto samplers and electron capture detectors (GC-ECD) were used.

Total organic carbon was measured on a Shimadzu-TOCV Total Organic Carbon Analyzer according to standard method 5310. UV absorbance at 254 nm ( $UV_{254}$ ) measurements were made with a Genesys 10s spectrophotometer. Chlorine concentration was measured either by the DPD titration method or by Hach method 8021 (DPD reagent).

Manganese measurements were made using a HACH field Mn kit (Hach method 8149, low range with PAN indicator) during column runs. Elemental media-oxide coating concentrations were measured on a Perkin Elmer Elan 9000 ICP-MS.

## **3.3 Results**

### **3.3.1 Column Study Water Quality Parameters**

A summary of column effluent water quality parameters for different runs is shown in Table 3.3 ( $Cl_2$  dose 3 mg/L, EBCT 1.4 min, HLR 4.2 gpm/ft<sup>2</sup>). The settled water had a Mn concentration of 0.34 mg/L (all of which was dissolved),  $UV_{254}$  absorbance of 0.038 cm<sup>-1</sup>, TOC and DOC concentrations of 3.1 mg/L and 2.7 mg/L, respectively, turbidity of 0.498 NTU, and pH of 6.6.

**Table 3.3. Summary of column effluent water quality parameters for different runs.**

Anthracite	Cl <sub>2</sub>	Water Type	UV <sub>254</sub> Abs (cm <sup>-1</sup> )	Turbidity (NTU)	Total Mn (HACH) (mg/L)
No	Pre	Settled	0.038	0.244	0.34
Coated	Pre	DI	0.006	0.202	0.02
Coated	Pre	Settled	0.036	0.190	0.05
Uncoated	Pre	DI	0.007	0.195	< 0.01
Uncoated	Pre	Settled	0.038	0.238	0.24
Coated	Post	DI	0.003	0.224	< 0.01
Coated	Post	Settled	0.038	0.203	0.07

Pre-chlorination using MnO<sub>x</sub> coated anthracite (from the Trap Falls WTP) resulted in an average Mn removal of 85.3 % and post-chlorination resulted in 83.5 % removal. The large Mn(II) removal with no pre-column chlorine can be attributed to Mn(II) adsorption to the MnO<sub>x</sub> coated media. The anthracite had a coating level of 82 mg Mn/g media, more than double the level of 35 mg Mn/g media previously measured by Islam et al. (2010) for the same WTP. The effluent Mn concentration with pre-column chlorination increased slowly over time from 0.04 mg/L after 2 minutes to 0.07 mg/L after 30 minutes; with no pre-column chlorine the Mn concentration increased from 0.05 mg/L after 2 minutes to 0.08 mg/L after 30 minutes and 0.10 mg/L after 1 hour and 15 minutes.

The average Mn removal with pre-column chlorine using uncoated anthracite (measured Mn coating level of 0.002 mg Mn/g media) was 29.4 %; the Mn concentration decreased from 0.28 mg/L after 2 minutes to 0.21 mg/L after 30 minutes. This steady decrease over time could be the result of Mn(II) sorption to accumulating media MnO<sub>x</sub>

followed by rapid catalytic oxidation by free chlorine. There was very little Mn decrease with pre-column chlorine but no granular media (an average of 1.5 %).

The largest average decrease in UV absorbance at 254 nm was also observed in the run with pre-column chlorination and MnO<sub>x</sub> coated media (0.038 cm<sup>-1</sup> to 0.036 cm<sup>-1</sup> with a minimum value of 0.035 cm<sup>-1</sup>). The average effluent TOC concentrations were similar for all runs with the settled water.

### **3.3.2 Column Study Disinfection Byproduct Formation**

Figure 3.3 shows instantaneous and 24 hour HAA<sub>5</sub> concentrations. Samples from runs with DI water had instantaneous HAA<sub>5</sub> and 24 hour concentrations of approximately 1 to 4 µg/L and 2 to 12 µg/L. These results suggest that there was a small amount of filter associated NOM with DBP formation potential. The instantaneous HAA<sub>5</sub> concentrations for runs with pre-column chlorinated settled water were similar for runs without media, with coated anthracite, and with uncoated anthracite. With the exception of the pre-chlorinated uncoated anthracite column 2 minute-effluent samples, instantaneous effluent concentrations for pre-chlorinated runs ranged from 11.4 µg/L to 12.7 µg/L. The average instantaneous HAA<sub>5</sub> concentrations for post-chlorinated samples were approximately 3 µg/L lower than those of corresponding pre-chlorinated samples. However, after holding the samples for 24 hours, the HAA<sub>5</sub> concentrations of the post-column chlorinated samples were similar to those of the pre-column chlorinated samples using MnO<sub>x</sub> coated anthracite, and these concentrations were approximately 3 µg/L lower than those in pre-chlorinated samples with no media or uncoated media.

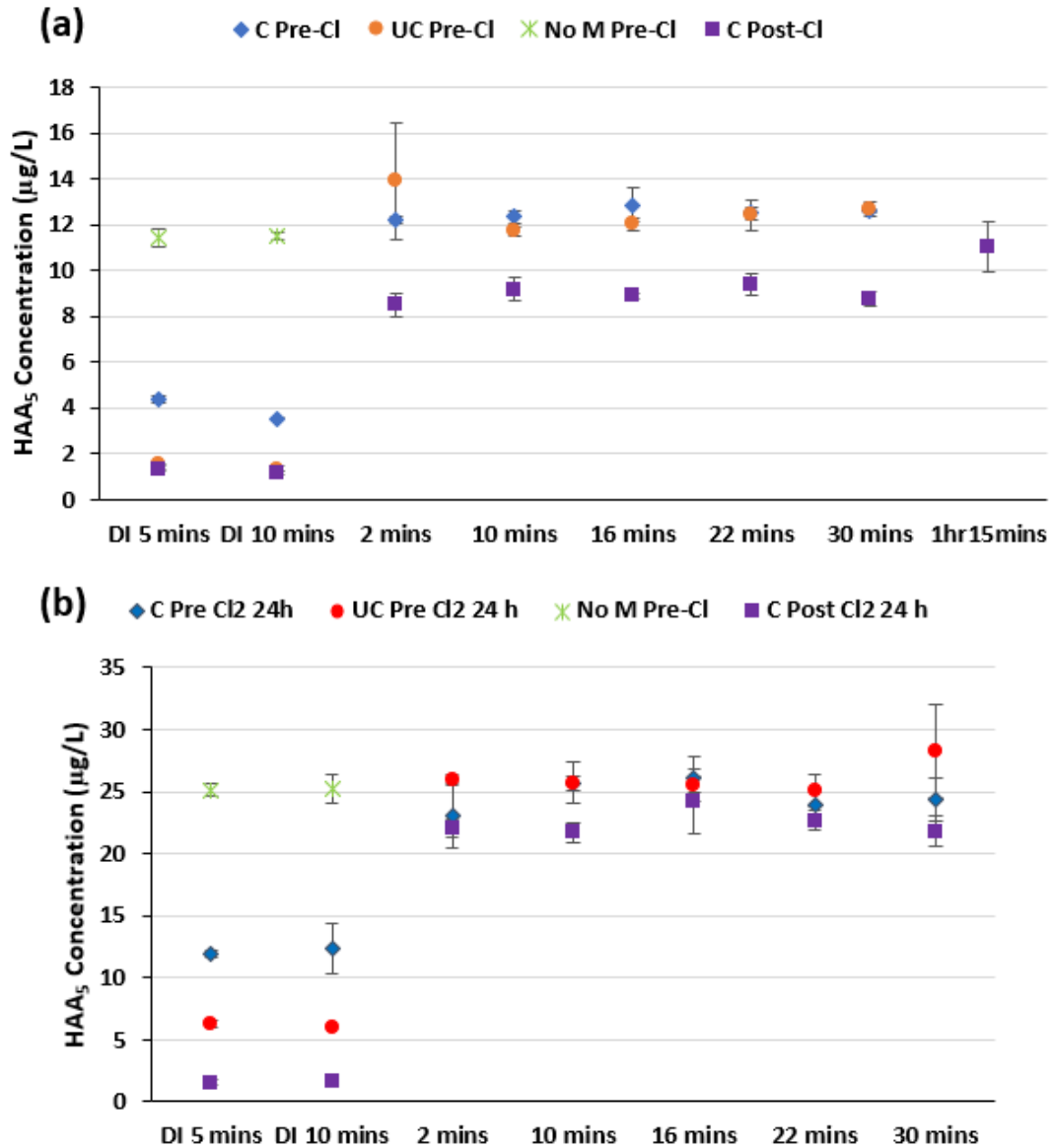


**Figure 3.3. Sample (a) instantaneous and (b) 24 hour HAA<sub>5</sub> concentrations.**

The TTHM concentrations are not reported due to a temporary failure in the chloroform measurement method. Average instantaneous effluent bromodichloromethane (BDCM), one of the four regulated trihalomethanes, concentrations were generally within 1 µg/L of each other for all column runs (no media, coated or uncoated media, pre- or post- chlorination). After 24 hours, BDCM concentrations were approximately 2 µg/L

lower in samples treated with pre-column chlorine and MnO<sub>x</sub> coated anthracite than in samples that underwent different treatment (Figure 3.4). The trends in instantaneous and 24-hour BDCM concentrations suggest that the MnO<sub>x</sub> coated anthracite removed slightly more precursors that require a longer reaction time to form BDCM.

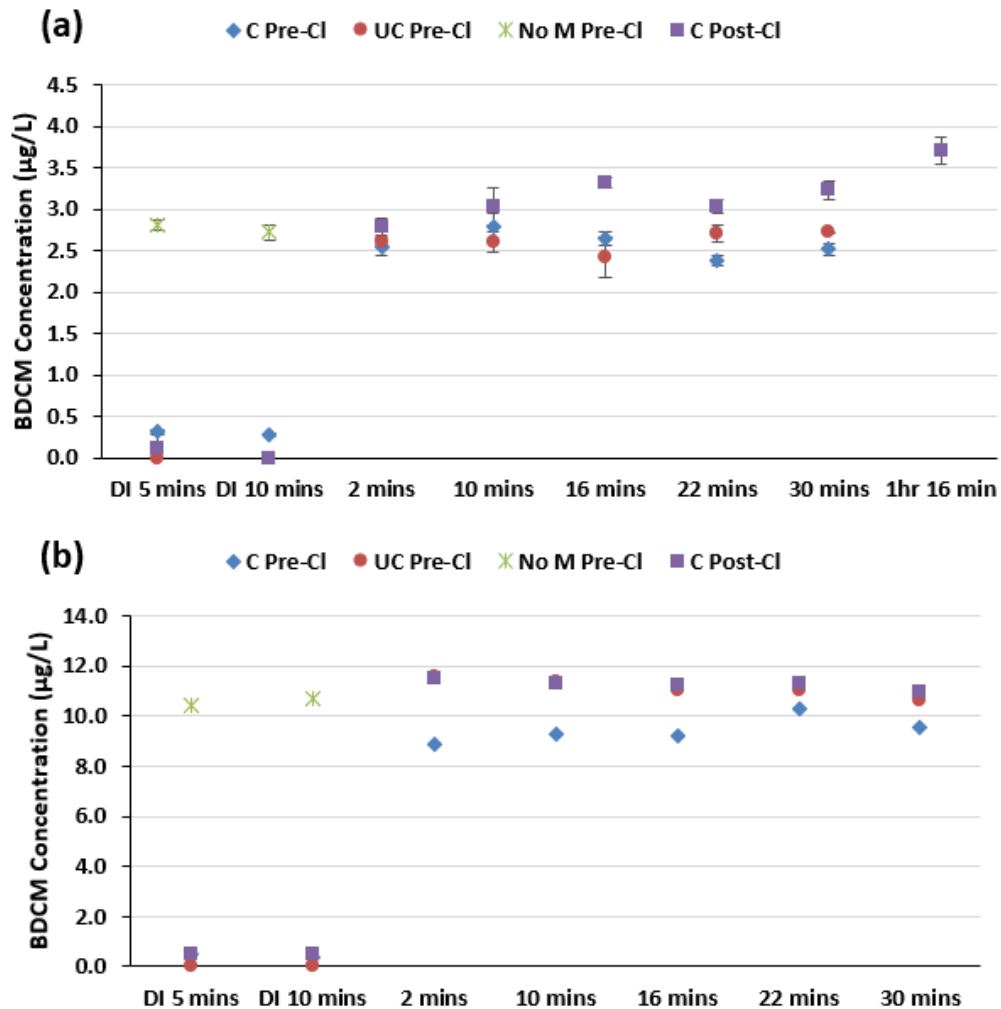


Figure 3.4. Sample (a) instantaneous and (b) 24 hour BDCM concentrations.

### 3.3.3 Full Scale Disinfection Byproduct Formation

Filter influent and effluent samples were collected from the Putnam WTP and Lantern Hill WTP, and held for 24 or 48 hours prior to DBP measurement to assess the potential impact of contact with MnO<sub>x</sub>-coated media on DBP formation. Putnam WTP samples were collected with and without pre-oxidant (ClO<sub>2</sub>) addition in the mixing basins (ahead of sedimentation and subsequent chlorination ahead of granular media filtration). The difference was calculated by subtracting the influent concentration from the effluent concentration, and dividing the difference by the filter influent concentration.

#### 3.3.3.1 Putnam WTP

Tables 3.4 and 3.5 show Putnam filter influent and effluent instantaneous HAA<sub>5</sub> and TTHM concentrations, their percentage of the 24-hour concentrations, and the percentage difference in concentrations from the influent to effluent.

**Table 3.4. Average instantaneous HAA<sub>5</sub> concentrations and percentages.**

No.	Date	Filter Influent		Filter Effluent		% Difference
		Inst. HAA <sub>5</sub> (µg/L)	% of 24-hr Conc.	Inst. HAA <sub>5</sub> (µg/L)	% of 24-hr Conc.	
1	2014 May	12.4	39%	26.0	73%	110%
2	2014 Aug*	14.3	37%	26.6	79%	86%
3	2014 Oct*	9.0	35%	21.0	79%	133%
4	2015 June	7.4	37%	19.9	81%	170%
5	2015 Oct*	9.0	35%	21.0	79%	133%
6	2015 Dec	5.3	23%	13.6	49%	155%
7	2016 April	16.1	50%	32.0	72%	99%
8	2016 May *	18.9	65%	35.1	100%	85%
9	2016 Sept*	20.5	39%	48.9	109%	139%
10	2017 June*	22.2	77%	31.3	101%	41%
<b>Average</b>		<b>13.5</b>	<b>44%</b>	<b>27.5</b>	<b>82%</b>	<b>115%</b>

\* indicates that pre-oxidation with chlorine dioxide was in use at the time of sample collection

The instantaneous concentrations were divided by the corresponding 24-hour concentrations of the samples and multiplied by one hundred to find their percentage of the 24-hour value. The EBCT for the sampling dates ranged from 9.9 to 18.8 minutes, with an average of 14.9 minutes.

Filter influent instantaneous HAA<sub>5</sub> concentrations ranged from 5.3 µg/L to 22.2 µg/L with an average of 13.5 µg/L. Effluent HAA<sub>5</sub> concentrations ranged from 13.6 µg/L to 48.9 µg/L with an average of 27.5 µg/L. The filter effluent HAA<sub>5</sub> concentrations were 41% to 170% greater than the influent concentrations. The greatest observed increase from influent to effluent concentrations did not occur for samples with the longest EBCT, and the smallest increase was not observed for the shortest EBCT. There was no visible trend in pre-oxidant use and DBP formation.

Influent instantaneous HAA concentrations were 44% of 24-hour concentrations on average with a range of 23% to 77%. Effluent instantaneous concentrations averaged 82% of 24-hour concentrations, ranging from 49% to 109%.

**Table 3.5. Average instantaneous TTHM concentrations and percentages.**

No.	Date	Filter Influent		Filter Effluent		% Difference
		Inst. TTHM (µg/L)	% of 24-hr Conc.	Inst. TTHM (µg/L)	% of 24-hr Conc.	
1	2014 May	26.7	42%	43.8	60%	64%
2	2014 Aug*	22.1	31%	43.5	65%	97%
3	2014 Oct*	11.6	33%	24.5	68%	111%
4	2015 June	13.3	28%	38.8	73%	192%
5	2015 Oct*	11.6	33%	24.5	68%	111%
6	2015 Dec	5.5	15%	22.9	48%	314%
7	2016 April	12.3	40%	25.7	65%	109%
8	2016 May *	19.6	52%	40.4	63%	106%
9	2016 Sept*	30.2	55%	30.2	64%	0%
10	2017 June*	17.7	67%	29.1	97%	64%
<b>Average</b>		<b>17.1</b>	<b>40%</b>	<b>32.3</b>	<b>67%</b>	<b>117%</b>

\* indicates that pre-oxidation with chlorine dioxide was in use at the time of sample collection

Filter influent instantaneous TTHM concentrations ranged from 5.5 µg/L to 30.2 µg/L with an average of 17.1 µg/L. Effluent TTHM concentrations ranged from 22.9 µg/L to 43.8 µg/L with an average of 32.3 µg/L. Effluent instantaneous TTHM concentrations were 117% greater than influent concentrations on average, ranging from no difference to a 314% increase from influent to effluent. There was no correlation between EBCT and TTHM increase from influent to effluent.

Influent instantaneous TTHM concentrations ranged from 15% to 67% of 24-hour, and averaged 40%. Effluent concentrations were 48% to 97% of 24-hour concentrations, with an average of 67% of 24-hour concentrations.

The average increase in concentrations from the influent to the effluent was similar for instantaneous HAA<sub>5</sub> and TTHM, though the range of increase was greater for TTHMs. DBP formation increases with increasing reaction time under favorable conditions (pH, temperature, chlorine residual, precursor concentration). The comparable

increases in DBP concentrations from the filter influent to effluent can be attributed to continuous formation over the EBCT ( $14.9 \pm 2.7$  minutes).

Examining instantaneous concentrations as percentages of 24-hour concentrations revealed that filter influent instantaneous HAA<sub>5</sub> and TTHM concentrations were  $44\% \pm 16\%$  and  $40\% \pm 15\%$ , respectively, of the corresponding 24-hour concentrations. Filter effluent instantaneous HAA<sub>5</sub> and TTHM concentrations were  $82\% \pm 17\%$  and  $67\% \pm 12\%$ , respectively, of the corresponding 24-hour concentrations. The average influent 24-hour percentage HAA<sub>5</sub> and TTHM concentrations were similar, and less than 50% of the 24-hour concentrations. The average effluent 24-hour percentage HAA<sub>5</sub> was 82% of the 24-hour concentrations, and was greater than that of the TTHMs (67%). These results suggest that a larger fraction of the measured 24-hour HAA<sub>5</sub> were formed within the residence time of the filters than the 24-hour TTHM.

Figure 3.5 shows HAA<sub>5</sub> and TTHM concentrations for 24-hour filter influent and effluent samples.

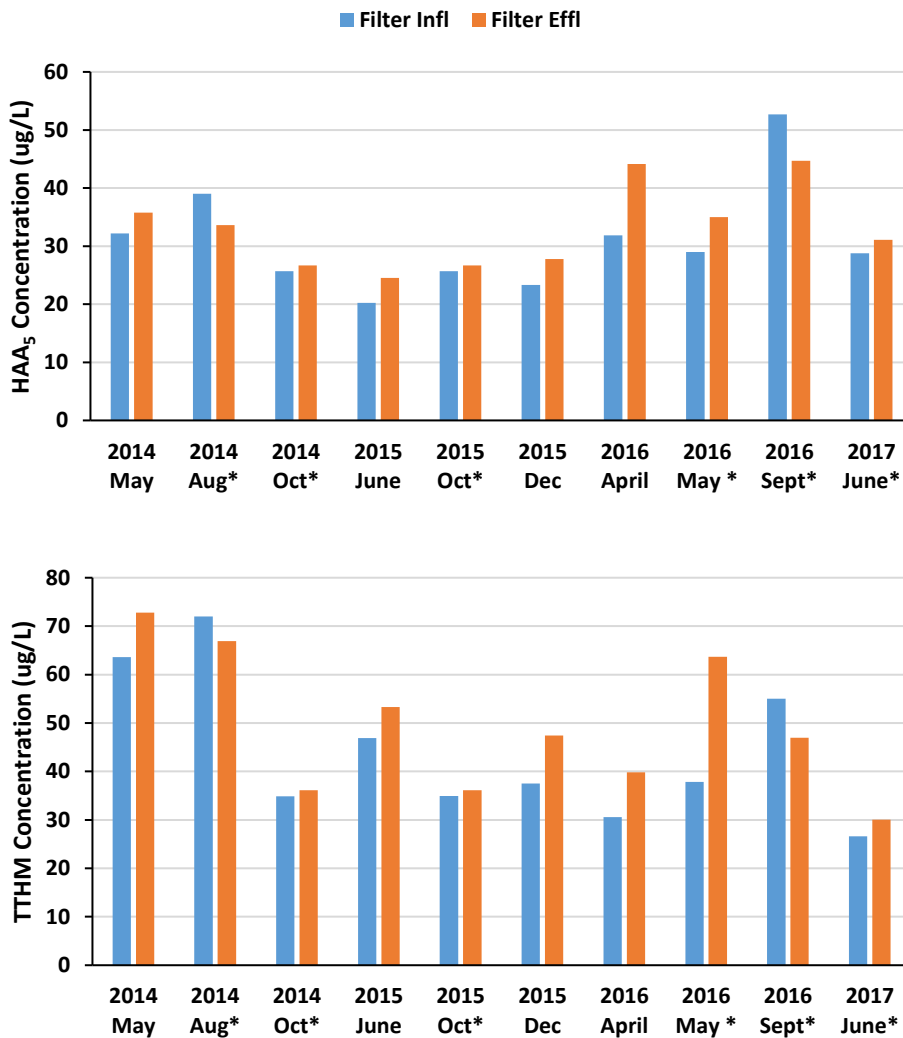


**Figure 3.5. Average (a) HAA<sub>5</sub> and (b) TTHM concentrations of filter influent and effluent samples held for 24 hours. \* indicates that pre-oxidation with chlorine dioxide was in use at the time of sample collection.**

Table 3.6 shows influent and effluent 24-hour DBP concentrations, and percentage differences between influent and effluent concentrations. The average absolute difference between filter influent and effluent HAA<sub>5</sub> and TTHM 24-hour concentrations was 16% and 19%, respectively. These percentage differences between

24-hour influent and effluent concentrations were significantly smaller than observed for instantaneous influent and effluent HAA<sub>5</sub> and TTHM concentrations (115% and 117%, respectively). Effluent 24-hour concentrations were greater than influent concentrations for all sampling dates but two, August 2014 and September 2016.

**Table 3.6. Average 24-hour DBP concentrations and percentage differences.**

Date	24-hr HAA <sub>5</sub> (µg/L)		% Difference	24-hr TTHM (µg/L)		% Difference
	Filter Infl.	Filter Effl.		Filter Infl.	Filter Effl.	
2014 May	32.2	35.8	11%	63.6	72.8	14%
2014 Aug*	39.0	33.6	-14%	72.0	66.9	-7%
2014 Oct*	25.7	26.7	4%	34.9	36.1	3%
2015 June	20.2	24.5	21%	46.9	53.3	14%
2015 Oct*	25.7	26.7	4%	34.9	36.1	3%
2015 Dec	23.3	27.8	19%	37.5	47.4	26%
2016 April	31.9	44.1	39%	30.6	39.8	30%
2016 May *	29.0	35.0	21%	37.8	63.7	68%
2016 Sept*	52.7	44.7	-15%	55.0	47.0	-15%
2017 June*	28.8	31.1	8%	26.6	30.0	13%
<b>Absolute Av</b>	<b>30.8</b>	<b>33.0</b>	<b>16%</b>	<b>44.0</b>	<b>49.3</b>	<b>19%</b>

\* indicates that pre-oxidation with chlorine dioxide was in use at the time of sample collection

Filter influent 24-hour HAA<sub>5</sub> and TTHM concentrations were approximately 2.5 and 3 times greater, respectively, than instantaneous concentrations. Effluent 24-hour HAA<sub>5</sub> and TTHM concentrations were approximately 1.3 and 1.5 times, respectively, greater than instantaneous effluent concentrations. As stated previously, this suggests that most of the DBP formation occurred within the EBCT of approximately 14.9 minutes, and a smaller amount of DBPs formed over the next 24 hours. The 24-hour filter influent HAA<sub>5</sub> and TTHM concentrations were relatively smaller than corresponding effluent concentrations, and this may be due to chlorine interacting with filter-media associated NOM as shown by Brown et.al. 2006.

### 3.3.3.2 Lantern Hill WTP

A similar examination of second stage contactor (SSC) influent and effluent at the Lantern Hill WTP (LHWTP) was performed. In the LHWTP (see Section 4.2.1), the majority of Mn(II) removal occurs across the SSCs, after iron and NOM removal across the dual media filters.

Tables 3.7 and 3.8 show SSC influent and effluent instantaneous HAA<sub>5</sub> and TTHM concentrations, their percentage of the 24-hour concentrations, and the percentage difference in concentrations from the influent to effluent. The EBCT for the sampling dates ranged from 2.2 to 3.0 minutes, with an average of 2.6 minutes.

**Table 3.7. Average instantaneous HAA<sub>5</sub> concentrations and percentages.**

No.	Date	SSC Influent		SSC Effluent		% Difference
		Inst. HAA <sub>5</sub> (µg/L)	% of 24-hr Conc.	Inst. HAA <sub>5</sub> (µg/L)	% of 24-hr Conc.	
1	2014 April	2.4	31%	3.6	47%	46%
2	2014 June	39.6	57%	41.8	65%	6%
3	2014 July <sup>+</sup>	20.3	37%	28.4	50%	40%
4	2014 Sept <sup>+</sup>	25.1	44%	29.2	60%	16%
5	2014 Oct <sup>+</sup>	22.4	42%	21.9	43%	-2%
6	2015 May	19.8	48%	20.5	55%	3%
7	2015 Aug	26.8	51%	25.4	53%	-5%
8	2015 Sept <sup>+</sup>	24.8	46%	25.4	47%	3%
<b>Average</b>		<b>22.7</b>	<b>44%</b>	<b>24.5</b>	<b>52%</b>	<b>15%</b>

<sup>+</sup>indicates where samples were held for 48 hours and not 24.

The SSC instantaneous influent and effluent HAA<sub>5</sub> concentrations were 22.7 ± 10.2 µg/L and 24.5 ± 10.7 µg/L respectively. Instantaneous effluent concentrations were 3% to 46% greater than influent HAA<sub>5</sub> concentrations. Effluent HAA<sub>5</sub> concentrations were 2% and 5% less than influent concentrations, respectively, for the October 2014 and September 2015 sampling dates.

Instantaneous TTHM influent and effluent concentrations were  $26.3 \pm 12.1 \mu\text{g/L}$  and  $31.2 \pm 12.5 \mu\text{g/L}$  respectively. Instantaneous effluent TTHM concentrations were 9% to 54% greater than corresponding influent concentrations. Effluent TTHM concentrations were 3% less than influent concentrations on the October 2014 sampling date. The two dates with larger observed instantaneous influent than effluent concentrations were two of three dates with the shortest EBCT of 2.2 minutes. Average absolute percentage differences between SSC influent and effluent HAA<sub>5</sub> and TTHM concentrations were relatively low, 15% and 22% respectively. The observed differences in HAA<sub>5</sub> and TTHM for the Putnam WTP were greater than 100%. The average EBCT for the LHWTP was less than a fifth (17%) of that of the Putnam WTP.

**Table 3.8. Average instantaneous TTHM concentrations and percentages.**

No.	Date	SSC Influent		SSC Effluent		% Difference
		Inst. TTHM ( $\mu\text{g/L}$ )	% of 24-hr	Inst. TTHM ( $\mu\text{g/L}$ )	% of 24-hr	
1	2014 April	14.3	23%	21.2	34%	48%
2	2014 June	54.6	57%	59.6	68%	9%
3	2014 July <sup>+</sup>	22.6	30%	34.7	49%	54%
4	2014 Sept <sup>+</sup>	19.8	40%	22.9	43%	16%
5	2014 Oct <sup>+</sup>	24.5	29%	23.8	30%	-3%
6	2015 May	22.3	41%	25.9	54%	16%
7	2015 Aug	29.0	39%	33.7	51%	16%
8	2015 Sept <sup>+</sup>	23.7	35%	27.6	37%	16%
	<b>Average</b>	<b>26.3</b>	<b>37%</b>	<b>31.2</b>	<b>46%</b>	<b>22%</b>

<sup>+</sup>indicates where samples were held for 48 hours and not 24

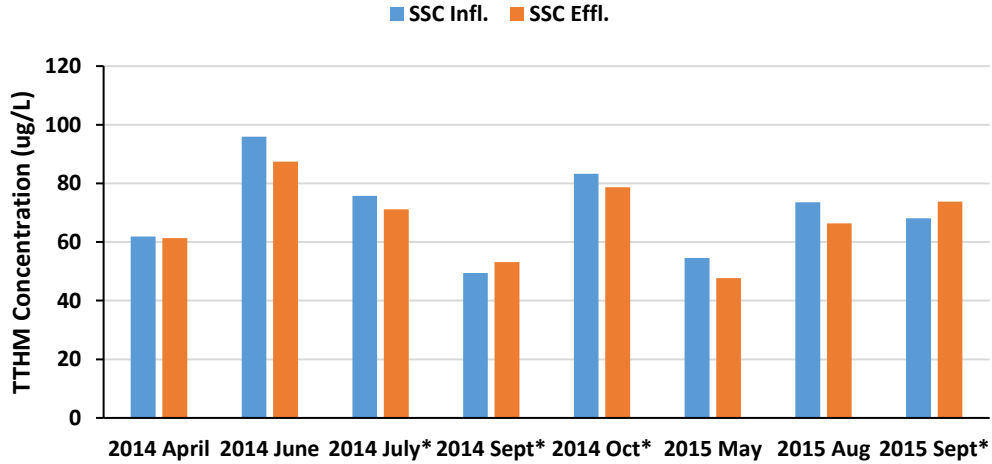
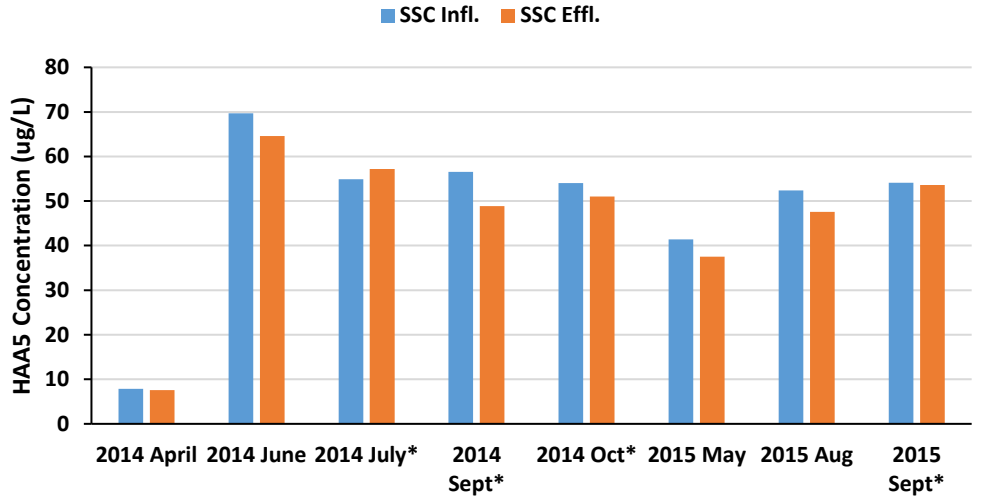
Influent SSC instantaneous HAA<sub>5</sub> and TTHM concentrations were approximately 44% and 37%, respectively, of corresponding 24-hour/48-hour concentrations. Effluent HAA<sub>5</sub> and TTHM concentrations averaged 52% and 46%, respectively, of corresponding 24-hour/48-hour concentrations.

Table 3.9 shows 24 and 48-hour DBP concentrations of influent and effluent samples. Twenty-four-hour SSC influent HAA<sub>5</sub> and TTHM concentrations were approximately 2 and 3 times, respectively, that of the instantaneous concentrations; effluent HAA<sub>5</sub> and TTHM 24-hour concentrations were both approximately twice the instantaneous concentrations.

**Table 3.9. Average 24-hour DBP concentrations and percentage differences.**

Date	24-hr HAA <sub>5</sub> (µg/L)		% Difference	24-hr TTHM (µg/L)		% Difference
	SSC Infl.	SSC Effl.		SSC Infl.	SSC Effl.	
2014 April	7.9	7.6	-4%	61.9	61.4	-1%
2014 June	69.6	64.6	-7%	96.0	87.5	-9%
2014 July <sup>+</sup>	54.9	57.2	4%	75.7	71.2	-6%
2014 Sept <sup>+</sup>	56.6	48.9	-14%	49.5	53.2	8%
2014 Oct <sup>+</sup>	54.0	51.0	-6%	83.3	78.7	-6%
2015 May	41.4	37.5	-9%	54.6	47.7	-13%
2015 Aug	52.4	47.6	-9%	73.6	66.4	-10%
2015 Sept <sup>+</sup>	54.1	53.6	-1%	68.1	73.7	8%
<b>Absolute Av</b>	<b>48.9</b>	<b>46.0</b>	<b>7%</b>	<b>70.3</b>	<b>67.5</b>	<b>7%</b>

<sup>+</sup>indicates where samples were held for 48 hours and not 24



**Figure 3.6. Average (a) HAA<sub>5</sub> and (b) TTHM concentrations of SSC influent and effluent samples held for 24 or 48 hours. \*indicates that samples were held for 48 hours.**

Figure 3.6 shows 24 and 48-hour SSC influent and effluent DBP concentrations. SSC influent 24-hour DBP concentrations were generally greater than SSC effluent 24-hour DBP concentrations. However, the average of the absolute differences for both HAA<sub>5</sub> and TTHM 24-hour concentrations was only 7%. This suggests that the MnO<sub>x</sub>-coated SSC media, with much less media associated NOM than a dual media filter for particle removal, did not impact DBP formation.

### 3.4 Conclusions

Laboratory column instantaneous HAA<sub>5</sub> concentrations for samples chlorinated post-column were lower than HAA<sub>5</sub> concentrations of samples chlorinated ahead of the columns. The 24-hour DBP concentrations of post-chlorinated samples were not significantly different than pre-chlorinated concentrations, suggesting that contact with the MnO<sub>x</sub>-coated media did not increase the potential of the water to form DBPs.

Instantaneous filter effluent DBP concentrations of samples from the Putnam WTP were approximately 116% greater than influent instantaneous concentrations. By comparison, instantaneous SSC effluent DBP concentrations of samples from the LH WTP were approximately 19% greater than influent instantaneous concentrations. One reason for observed percentage differences is the EBCT for reactors at the WTPs. The EBCT of the Putnam WTP filter is approximately 15 minutes, while that of the LH SSCs was approximately 2.6 minutes.

Putnam influent HAAs and TTHMs were approximately 40% of 24-hour influent concentrations, while effluent HAAs and TTHMs were approximately 75% of 24-hour influent concentrations. These results show that 40% of the 24-hour effluent DBP concentrations formed from the point of chlorine addition to the filter influent sample collection location, and 35% of the 24-hour effluent DBP concentrations formed within the 15 minutes from filter influent to effluent. The average difference between influent and effluent 24-hour DBP concentrations for samples from Putnam WTP and LHWTP were approximately 17% and 7% respectively. When the samples were allowed to react for 24 hours, the difference in reaction times for influent versus effluent samples was

much smaller, leading to smaller differences between influent and effluent 24-hour DBP concentrations.

The 24-hour filter influent HAA<sub>5</sub> and TTHM concentrations were relatively smaller than corresponding effluent concentrations for samples from the Putnam treatment plant which practices Mn(II) removal across MnO<sub>x</sub>-coated dual media filters. This may be due to chlorine interacting with filter-media associated NOM as shown by Brown et.al. 2006. The absolute differences for both HAA<sub>5</sub> and TTHM 24-hour and 48-hour SSC influent and effluent DBP concentrations at the Lantern Hill treatment plant was marginal (7%), with the SSC effluent concentrations exceeding influent concentrations for some samples. This suggests that the MnO<sub>x</sub>-coated SSC media, with much less media associated NOM than a dual media filter for particle removal, showed even less of an impact on DBP formation, consistent with column study results which showed that MnO<sub>x</sub> surfaces did not have a significant impact on DBP formation.

## CHAPTER 4

# FULL-SCALE IMPLEMENTATION OF SECOND-STAGE CONTACTORS FOR MANGANESE REMOVAL<sup>1</sup>

### 4.1 Introduction

The presence of manganese (Mn) in distributed drinking water may lead to operational problems and consumer complaints due to aesthetic quality concerns (discolored water, staining of fixtures). The biochemical reduction of Mn-containing minerals in aquifers and reservoir sediments under anoxic conditions can result in elevated levels of dissolved manganese (Mn(II)) in source waters. The United States Environmental Protection Agency (EPA) set a secondary maximum contaminant level (SMCL) of 0.05 mg/L to control taste, odor and color complaints by consumers (USEPA (1992)), and a lifetime health advisory of 0.3 mg/L in water to address potential neurological effects (USEPA (2004)). However, the recommended treatment goal to avoid operational and chronic problems such as water discoloration, turbidity, and scaling in pipes and valves is 0.01 to 0.02 mg/L (Brandhuber et al. (2013); Kohl and Medlar (2006); Sly, Hodgkinson and Arunpairojana (1990)). The Canadian Federal-Provincial-Territorial Committee on Drinking Water (CDW) recently published an updated drinking water guideline for manganese for public consultation. The guideline proposes a maximum acceptable concentration (MAC) of 0.1 mg/L based on neurological effects

---

<sup>1</sup> Modified from originally published version (Bazilio, A. A., Kaminski, G. S., Larsen, Y., Mai, X., & Tobiason, J. E. (2016). Full-scale implementation of second-stage contactors for manganese removal. *Journal-American Water Works Association*, 108(12), E606-E614.)

observed in rodents, and an aesthetic objective (AO) of 0.02 mg/L for total manganese in drinking water (Health Canada (2016)).

Manganese control strategies most commonly practiced include: 1) oxidation and precipitation by a strong oxidant (e.g. permanganate, chlorine dioxide, or ozone) ahead of particle removal, and 2) sorption of dissolved Mn(II) to manganese oxide coated porous media in conjunction with catalytic oxidation by free chlorine. The latter method exhibits very rapid oxidation of surface bound Mn(II) in the pH range of most waters, and results in regeneration of the manganese oxide ( $\text{MnO}_{x(s)}$ ) coating (Knocke, Occiano and Hungate (1991)). In contrast, homogenous oxidation of dissolved Mn(II) by free chlorine ( $\text{HOCl}$ ,  $\text{OCl}^-$ ) is slow at typical drinking water treatment pH, time, and temperature conditions (Knocke, Hoehn and Sinsabaugh (1987)). The Mn(II) adsorption capacity of  $\text{MnO}_x$  coated media increases with increased surface  $\text{MnO}_x$  concentration, influent chlorine concentration, and solution pH (Tobiason et al. (2008); Knocke, Occiano and Hungate (1991); Morgan and Stumm (1964)). A measure of the Mn(II) uptake capacity of  $\text{MnO}_x$  coated filter media from several drinking water treatment plants (Islam et al. (2010)) showed a general non-linear increase in Mn(II) uptake with increasing  $\text{MnO}_x$  coating level (mg Mn/g media). A continuously present free chlorine residual allows regeneration of surface sites and prevents Mn release at a pH of 6.5-7.1 (Gabelich et al. (2006); Knocke, Occiano and Hungate (1990)).

Halogenated disinfection byproducts (DBPs) may form during treatment when chlorine or other disinfectants react with natural organic matter (NOM) in water. Some DBPs are known to be carcinogenic and genotoxic. Total trihalomethanes (TTHM) and five haloacetic acids ( $\text{HAA}_5$ ), all halogenated organic compounds, are regulated by the

EPA at maximum contaminant levels (MCLs) of 0.080 mg/L and 0.060 mg/L, respectively. Stage 2 of the Disinfectants and Disinfection Byproducts Rule (USEPA (2006)) stipulates that locational running annual averages for each monitoring location in the distribution system meet these limits. The nine regulated compounds are only a small fraction of DBPs that have been identified to date, and studies show that other unregulated DBPs may be more genotoxic than those currently regulated (Richardson et al. (2007b)). As the occurrence and toxicity of unregulated DBPs become better understood, there may be new regulation of these compounds.

While effective for Mn(II) removal, adding chlorine ahead of dual media (DM) filtration for catalytic oxidation can increase DBP concentrations as compared to chlorination after DM filtration (Tobiason et al. (2008); Brown (2006); Corbin et al. (2003)). Corbin et al. (2003) examined the effect of adding chlorine post filtration instead of pre-filtration on DBP concentrations for three water treatment plants in Connecticut, USA. Samples were held for the average clear-well residence time plus 24 hours for simulated distribution system samples (SDS). SDS samples showed annual average decreases of up to 32% and 27% in HAA<sub>5</sub> and TTHM concentrations respectively, with the greatest decreases observed in the spring. However, the authors noted that post-filtration chlorination at plants with high seasonal iron and manganese concentrations would only be feasible if metals removal was achieved by alternative methods (i.e., not pre-oxidation or sorption and catalytic oxidation across MnO<sub>x</sub> coated granular media primarily designed for particle removal).

The use of second stage contactors (SSCs) for Mn(II) removal by sorption and surface oxidation by free chlorine after particle removal by granular media filtration has

been examined at laboratory and pilot scales (Chihoski (2012); Knocke et al. (2010); Tobiasson et al. (2008)). Having the sorption and catalytic oxidation process for Mn(II) removal after particle filtration minimizes DBP formation, probably by minimizing the contact of free chlorine with raw water and media associated NOM. The SSC configuration using MnO<sub>x</sub>-coated media coarser than traditional filter media (2.0 to 2.5 mm versus 0.5 to 1 mm diameter) successfully removed influent Mn(II) concentrations of 0.02 to 0.3 mg/L at high HLR of 16 to 24 gpm/ft<sup>2</sup>, over a wide pH range. A free chlorine residual of at least 1.0 mg/L as Cl<sub>2</sub> was necessary, and removal was greater at pH 7.0 -8.0 than at pH 6.3-6.7 (Knocke et al. (2010)).

The Lantern Hill Water Treatment Plant (LHWTP) in Stonington, CT, USA treats a ground water source with 1.5- 2.5 mg/L of iron (Fe), 0.15-0.25 mg/L of Mn, 3- 4 mg/L of total organic carbon (TOC), and an average pH of 6.5. Prior to 2013, the plant employed a single stage of three parallel dual media filters (21 in of anthracite over 24 in of MnO<sub>x</sub> coated glauconite) in a direct filtration treatment train. A high pre-filter chlorine dose was added for Fe oxidation and precipitation ahead of DM filtration as well as maintenance of a significant free chlorine residual across the DM for Mn removal and for plant effluent free chlorine residual; pre-filter permanganate addition was also practiced which resulted in oxidation of some of the raw water Mn prior to the filter. The level of pre-filter chlorination resulted in elevated levels of DBPs due to the reaction of chlorine with the raw water NOM. A desire to pump the groundwater once only and the use of a single stage of direct filtration limited the treatment options. Lowering the pre-filter chlorine dose (and adding post-filter chlorination for the distribution residual target) resulted in lower DBP concentrations but was accompanied by increased effluent Mn

concentrations after 45 days of operation (Russell (2008)), most likely due to release of Mn from the filter media due to microbiological reduction (Islam et al. (2010)).

Addition of a second stage contactor was considered in order to achieve manganese removal without forming high levels of DBPs. Pilot studies in the laboratory and on-site were conducted to test SSC performance for this system. On-site studies using a two-stage pilot-scale filter system showed that a SSC with a 40 in pyrolusite (an MnO<sub>2</sub> mineral) media bed, after iron and some TOC removal by dual media filtration, successfully removed Mn(II) and resulted in 60 and 80% decreases in TTHM and HAA<sub>5</sub> concentrations in effluent samples held for 24 hours (Pham (2010)). Chihoski (2012) tested the performance of different types of SSC media including MnO<sub>x</sub> coated anthracite, MnO<sub>x</sub> coated Macrolite, and pyrolucite. Manganese oxide coated Macrolite M7 performed best at a HLR of up to 20 gpm/ft<sup>2</sup> and a free chlorine residual of approximately 1 mg/L, producing effluent Mn concentrations of ≤0.01 mg/L. Macrolite M7 is a synthetic porous ceramic media (Fairmount Water Solutions, Chardon, Ohio) with an average grain density of 1.4 g/cm<sup>3</sup>. Using carefully dosed pre-filter chlorine for Fe(II) oxidation only, and post-filter chlorine for oxidation of SSC sorbed Mn(II) and system residual resulted in 59 and 58 % decreases in the 24 hour hold values for THMs and HAAs, respectively, compared to the existing full-scale plant. In comparison, pre-permanganate oxidation of iron used with post-filter chlorine resulted in 63 and 61 % decreases in THMs and HAAs, respectively.

The Aquarion Water Company (AWC) contracted with Tighe & Bond Engineers (Westfield, Mass.) to design an upgrade of the LHWTP based on results of the pilot

studies. The new LHWTP with rebuilt dual media filters and added second stage contactors went online in July 2013.

The objective of this paper is to document the performance of the full-scale plant with respect to iron and manganese removal and control of DBPs, with special emphasis on the second stage contactors. The treatment approach taken is unusual, perhaps the first application of this particular sequence and operation of treatment processes.

## **4.2 Materials and Methods**

### **4.2.1 The full-scale plant**

Figure 4.1 shows a schematic of the 700 GPM capacity updated LHWTP. Sodium hydroxide (NaOH) is added to the raw water to increase the pH from approximately 6.3 to 7.3. A sub-stoichiometric dose of sodium hypochlorite (NaOCl) is added to oxidize the dissolved iron for removal by the DM filters. There is the option to use potassium permanganate (KMnO<sub>4</sub>) as a pre-oxidant. Cationic polymer, C-572 (Superfloc C-500 series, Kemira, Atlanta, Ga.), is also added to the raw water to increase TOC removal and aid particle retention by the DM filters.

Steel vessels were reused for the three parallel dual media filters, each containing 25 in of approximately 1 mm effective size (ES) anthracite (uniformity coefficient (UC) of 1.41) over 20 in of approximately 0.5 ES mm silica sand (UC = 1.37). The filters have a design HLR of 3 gpm/ft<sup>2</sup>, with backwash and air scour capability.

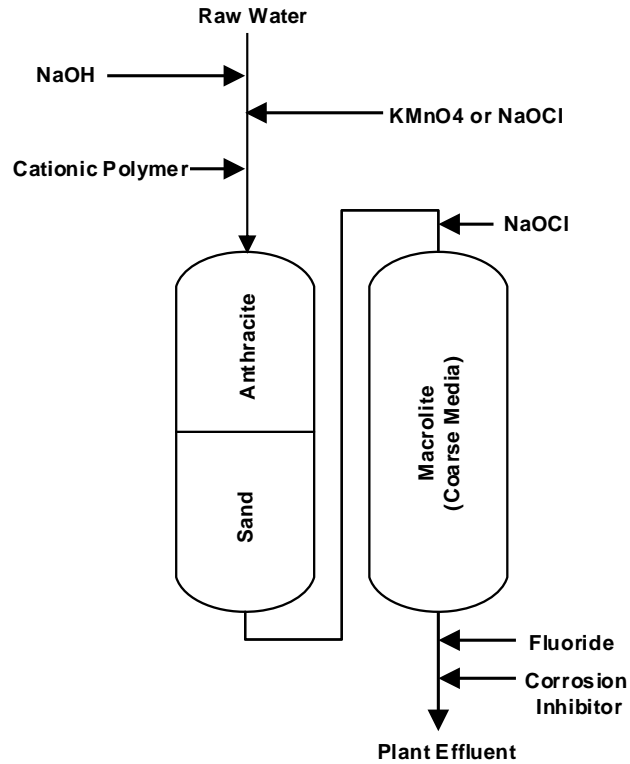
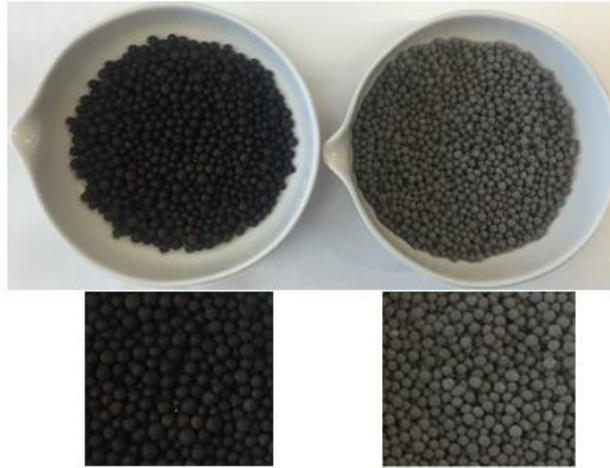


**Figure 4.1. Schematic of reconstructed LHWTP.**

Dual media filter effluent is dosed with sufficient sodium hypochlorite (NaOCl) to achieve catalytic manganese oxidation plus a plant effluent residual of approximately 1 mg/L as  $\text{Cl}_2$ , and then enters three parallel second stage contactors. Each SSC contains approximately 40 inches of 2 mm ES Macrolite M7 ( $\text{UC} = 1.2$ ). The M7 was coated with  $\text{MnO}_x$  in the vessels prior to plant startup using a procedure provided by a consultant (Derek French, Wateropolis Inc., Toronto, Ont.). Media were exposed to a 3% manganous sulfate ( $\text{MnSO}_4$ ) solution followed by a 2% potassium permanganate solution, with 30 minutes of air mixing followed by 30 minutes of soaking after the application of each solution, draining of the  $\text{MnSO}_4$  prior to  $\text{KMnO}_4$  soaking, and rinsing with 2 bed volumes of water after  $\text{KMnO}_4$  application. The sequence of alternate solutions was performed three times. The coating procedure was evaluated in the

laboratory prior to field implementation using uncoated M7 obtained from LHWTP to determine potential media  $\text{MnO}_x$  coating levels. Photographs of uncoated M7, and M7 coated at the plant by the above procedure are shown below.



**Photographic images of field- $\text{MnO}_x$  coated (left) and uncoated (right) Macrolite M7 media**

The contactors were designed for a HLR of 10 GPM/ft<sup>2</sup>. Water and air backwash options are included for the SSCs for fluidized backwash based removal of accumulated  $\text{MnO}_x$  on the media. Fluoride and corrosion inhibitor (blended phosphates) are added to SSC effluent, and there is the option to add additional chlorine for the distribution system residual.

#### **4.2.2 Field sampling**

Samples were collected across the plant during SSC backwash events for onsite bench measurements or analyses at the University of Massachusetts. Raw water, dual media filter influent and effluent, contactor influent and plant effluent samples were collected for metals, turbidity, free chlorine residual, organic carbon, and DBP measurements. Samples were separated onsite into particulate, colloidal, and dissolved fractions for iron and manganese measurements after Carlson et al. (1997). Samples

were syringe filtered with a 25 mm diameter 0.2  $\mu\text{m}$  track-etched Nuclepore polycarbonate membrane filter (Whatman, Clifton, N.J.), and with a Millipore regenerated cellulose 30 kDa nominal molecular weight cutoff membrane ultra-filter (UF) (Billerica, Mass.) in a 200 mL Amicon UF cell (Beverly, Mass.) with stirring under nitrogen at 30 psi. The particulate fraction is that which does not pass through the 0.2  $\mu\text{m}$  filter, the colloidal fraction passes through the 0.2  $\mu\text{m}$  filter but not the 30 kDa UF, and the dissolved fraction passes through the 30 kDa UF.

Samples for instantaneous DBP measurement were quenched upon collection, and samples for 24 and 48 hr. simulated distribution system (SDS) assessment were collected headspace free in BOD bottles, kept in the dark at 12  $^{\circ}\text{C}$ , and quenched after 24 and 48 hours respectively. Ammonium chloride was used to quench samples for THM analysis, and sodium sulfite to quench samples for HAA analysis.

The second stage contactors underwent high-rate backwash approximately every 6-8 weeks. Air-scouring was employed periodically during backwash, as discussed in the Results section. Contactor backwash was initiated after DM filter backwash and stabilization of plant effluent water quality. Composite backwash samples for each contactor were collected for Mn mass balance calculations. A 62 inch grain sampler (Best Harvest Farm and Home Testing Equipment, Largo, Fla.) with 10 sample slots was used twice (February 2014 and September 2015) to obtain SSC media samples for  $\text{MnO}_x$  coating depth profile assessment.

Water quality data (water production, Mn and Fe levels across the plant, turbidity, etc.) were also provided by the utility. Utility personnel made bench-top measurements of metals, free chlorine residual, pH,  $\text{UV}_{254}$ , and turbidity three times weekly.

### **4.2.3 Analytical methods.**

#### **4.2.3.1 Field measurements**

Manganese and iron were measured using Hach method 8149 (low range with PAN indicator) and 8008, respectively, and the corresponding field spectrophotometers (Hach Pocket Colorimeter II <sup>TM</sup> Manganese, and Iron (FerroVer®) kits, Hach, Loveland, Colo.). Free chlorine was measured by Hach method 8021 (DPD reagent). A Hach 2100 N turbidimeter (Hach, Loveland, Colo.) was used for benchtop turbidity measurements.

#### **4.2.3.2 Laboratory measurements**

Metal measurements were made using a Perkin Elmer Elan 9000 inductively coupled plasma mass spectrometer (ICP-MS) (Waltham, Mass.). Total and dissolved organic carbon were measured in accordance with Standard Methods (APHA, AWWA and WEF (1998)) method 5310 using a Shimadzu TOC-VCPH total organic carbon analyzer (Shimadzu, Kyoto, Japan). Total trihalomethane concentration was determined using the EPA 551.1 method (USEPA (1990)), and HAA<sub>5</sub> concentration using the EPA 552.2 method (USEPA (1995)) with minor modifications. Separation and detection were performed with Agilent Technologies 6890 Network gas chromatographs (GC) equipped with auto-samplers (Santa Clara, Calif.), capillary columns (DB-1, 30 m x 0.25 mm ID, 1.0 µm film thickness for HAAs, and DB-5, 30 m x 0.25-mm I.D, 1.0 µm film thickness for THMs), and an electron capture detector (ECD). The temperature program used for HAA analysis was the same published by Brophy, Weinberg and Singer (2000).

#### **4.2.4 Media and backwash particle characterization**

Contactors media MnO<sub>x</sub> coating levels (mg Mn/g Media) were determined using the method published by Knocke, Occiano and Hungate (1990). Approximately 1 g

samples of dried media were subjected to reductive dissolution using hydroxylamine sulfate (HAS) and 250 mL of 2% by volume of trace metal grade nitric acid. Composite contactor backwash samples were similarly digested with approximately 1 g HAS of per 250 mL of backwash and 2% nitric acid. The resulting extract solution was diluted and analyzed by ICP-MS for Mn and other metals.

Scanning electron microcopy (SEM) (Zeiss EVO 50 SEM, Zeiss, Jena, Germany) was performed on the MnO<sub>x</sub> coated media and MnO<sub>x</sub> particles of the composite contactor backwash sample. Samples were first dried for 48 hours at 60 °C, then mounted onto carbon tape and sputter coated (Edwards Xenosput XE200, Edwards, Inc., Tewksbury, Mass.) with platinum. The oxidation state of Mn in the backwash MnO<sub>x</sub> was determined by X-ray photoelectron spectroscopy (XPS) (Phi Quantum 2000 spectrometer, Physical Electronics Inc. (a division of ULVAC-Phi), Chanhassen, Mn.) after Cerrato et al. (2010).

X-ray diffraction (PANalytical X'Pert PRO X-ray diffraction system, PANalytical Inc., Westborough Mass.) was performed on freeze dried as well as suspended particles (in water) from contactor backwash.

### **4.3 Results**

From its startup in July 2013 to September 2015, the plant flow rate ranged from 250 gpm to 690 gpm as determined by AWC personnel; the AWC Mystic System demand varies seasonally and is met by the 2 MGD Deans Mill surface water treatment plant, the 1 MGD Lantern Hill WTP, and an interconnection with the Groton, CT system. The LHWTP plant was offline from December 23<sup>rd</sup> 2013 to March 11<sup>th</sup> 2014 to complete construction. Overall, the new treatment train has performed very well. Metals and TOC

removal were successful, and effluent DBP concentrations were low. Specifics of process performance are described below.

#### **4.3.1 Dual media filtration: turbidity, iron and NOM removal**

The filter influent chlorine dosing objective is to achieve a dissolved iron concentration of less than about 0.04 mg/L entering the DM filters while leaving no free chlorine residual. Cationic polymer was also added to the influent for NOM precipitation ahead of the filters and to aid in controlling particle breakthrough. Dual media filter effluent turbidity was typically less than 0.1 NTU with turbidity breakthrough occurring earlier (< 24 hours) during periods of high flow. Iron removal was complete across the DM filters (Figure 4.2) except in instances where particle breakthrough occurred. Filter effluent Fe concentrations were less than 0.02 mg/L on average when breakthrough did not occur. When DM filter breakthrough occurred, some iron was removed by the SSCs (up to 0.3 mg/L Fe) but not all as the SSCs are not designed for particle removal. Iron concentrations in the SSC backwash were elevated when these incidences occurred. As expected, very little Mn removal occurred across the DM filters, at only 0.03 to 0.04 mg/L Mn.

Decreases in total organic carbon ranged from 1 to 2.5 mg/L TOC across the DM filters with no significant TOC removal observed across the SSCs. The  $UV_{254}$  of the raw water was 0.16 to 0.18  $cm^{-1}$  and decreased to 0.04 to 0.06  $cm^{-1}$  in the filter effluent.

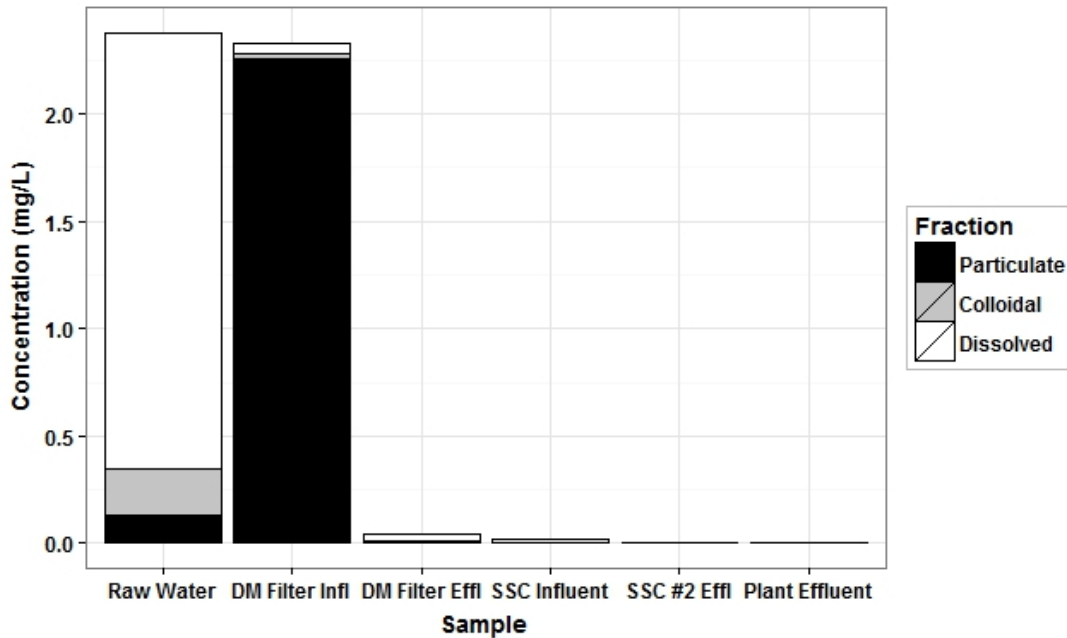


**Figure 4.2. Iron fractionation across the plant on August 27th, 2013.**

The DM filters were backwashed approximately every 24 hr. using effluent from two filters to backwash the third, with a filter-to-waste period at the end of backwash. The entire filter backwash sequence duration was approximately 1.5 hr. and there was no flow through the second stage contactors during this period. Initially after plant start-up, recurring drops in plant effluent free chlorine residual were observed after DM filter backwash. This was attributed to chlorine demand exerted for oxidation of media adsorbed Mn(II) in the contactors during the period of no flow (and thus no new influent chlorine). An increase in Mn with a decrease in Cl<sub>2</sub> residual in contactor to waste flow as seen in Figure 4.3 supports this hypothesis. To address the low effluent Cl<sub>2</sub> residual, the plant operation was changed to include a contactor-to-waste period for about 10 minutes after completion of the DM filter backwash.

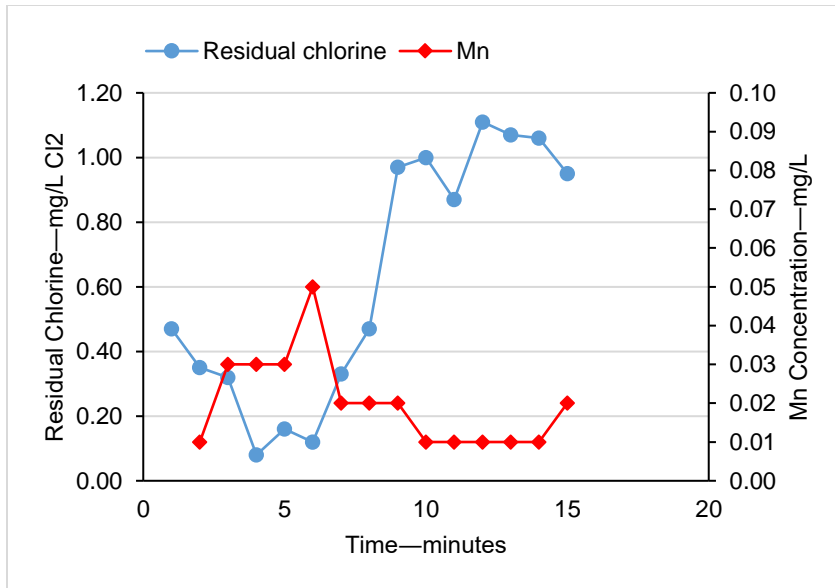


**Figure 4.3. Contactor to waste Mn and residual chlorine concentrations post DM filter backwash on November 11th, 2013.**

#### 4.3.2 Disinfection byproducts

Effluent DBP concentrations for the redesigned LH plant were significantly lower than for the original LH plant (Figure 4.4). The average HAA<sub>5</sub> and TTHM effluent concentrations from July 2013 to September 2015 were 32.0 µg/L and 31.7 µg/L respectively, well below their respective MCLs of 60 µg/L and 80 µg/L. The standard deviations were also low, 10 µg/L and 12 µg/L for HAA<sub>5</sub> and TTHM respectively.

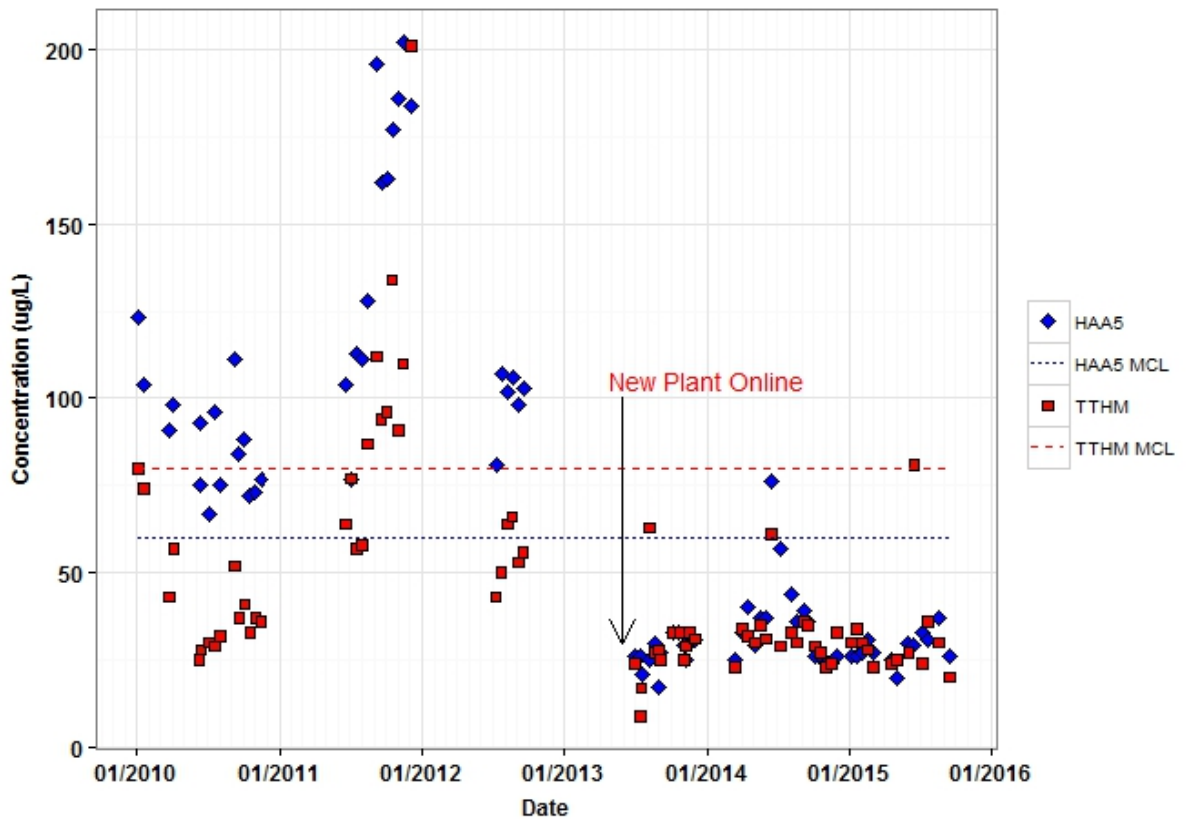


**Figure 4.4. Plant Effluent DBP concentrations from 2010 to 2015.**

Measurement of DBPs across the plant showed an increase in DBP concentration as shown in Figure 4.5 for August 29<sup>th</sup> 2013; the pre-filter chlorine dose was 3.01 mg/L and the contactor influent dose was 3.94 mg/L. Plant effluent simulated distribution system samples (SDS) held for 24 and 48 hr. had relatively low DBP concentrations. Both 24 and 48 hr. HAA<sub>5</sub> concentrations were below the HAA<sub>5</sub> MCL; the 24 hr. sample TTHM concentration was below the TTHM MCL, and the 48 hr. sample was just above at 81.3 µg/L.

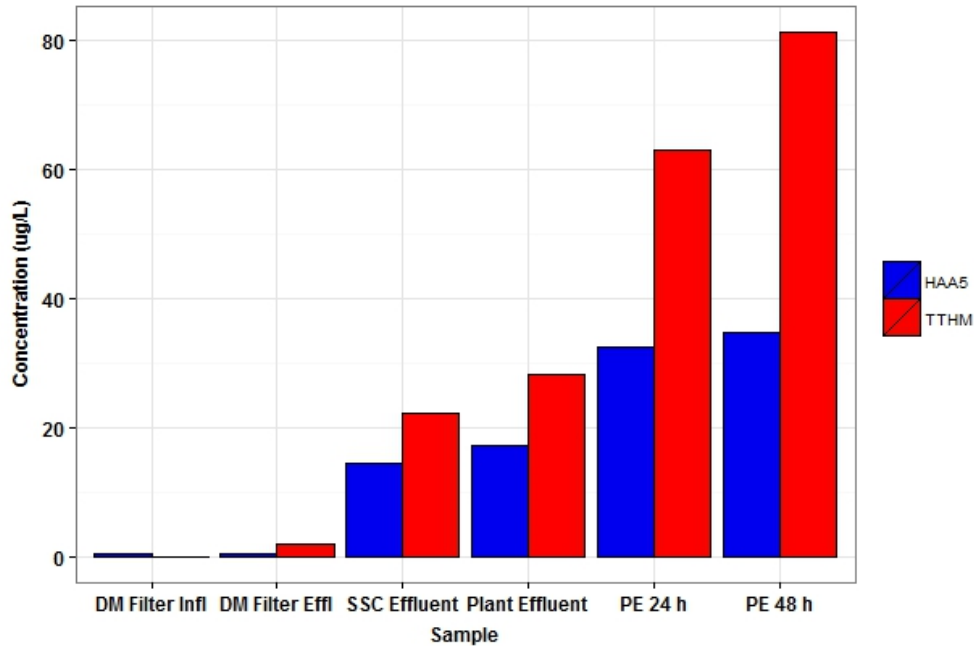


**Figure 4.5. Instantaneous across the plant, and 24 and 48 hr. SDS DBP concentrations on August 29th, 2013.**

When the pre-filter chlorine dose was optimal, sufficient only for Fe(II) oxidation and leaving no residual, TTHM and HAA<sub>5</sub> concentrations were typically lowest in the DM Influent. When the pre-filter chlorine dose was higher than the optimal dose, higher DBP concentrations resulted. For example a pre-filter dose of 6.8 mg/L Cl<sub>2</sub> as compared to the average dose of 3.8 mg/L Cl<sub>2</sub> resulted in DM Influent HAA<sub>5</sub> and TTHM concentrations of 19 µg/L and 22 µg/L, and plant effluent HAA<sub>5</sub> and TTHM concentrations of 36 µg/L and 63 µg/L. Examination of available data showed no significant association between plant effluent DBP concentrations and DM influent UV<sub>254</sub> absorbance, DM effluent UV<sub>254</sub> absorbance, or plant effluent TOC concentration.

The plant is designed to employ pre-filter potassium permanganate (KMnO<sub>4</sub>) which eliminates possible chlorine overdose and delays chlorine addition to post-filtration, potentially decreasing DBP formation as observed by Corbin et al. (2003).

However, practicing pre-filter Fe oxidation with  $\text{KMnO}_4$  would add operational complexity of using a second oxidant, present the possibility of overdosing resulting in post-DM filter permanganate that may create downstream concerns, and increase the overall amount of Mn in the treatment plant residuals.

### **4.3.3 Second stage contactors.**

#### **4.3.3.1 Mn removal**

Fractionation of Mn across the plant shows the forms of Mn and where removal occurs (Figure 4.6). Raw water Mn is nearly all dissolved, and DM filter effluent Mn is all dissolved with about 10 to 20% removal across the filter, probably by association with precipitated iron particles. This is expected based on pre-filter oxidant dosing intended for Fe oxidation only and no free chlorine residual available for development of an  $\text{MnO}_x$  coating on the DM filter media. As designed, 80 to 90% of the Mn removal occurred across the SSCs. The Mn concentration entering the SSCs was approximately 0.14 mg/L and effluent Mn concentrations were typically at or below the field method detection limit of 0.01 mg/L. The average contactor influent chlorine dose was 3.8 mg/L  $\text{Cl}_2$  and the pH ranged from 7.2 to 7.4. The average free chlorine residuals entering and leaving the SSCs were 1.5 and 0.9 mg/L  $\text{Cl}_2$ , respectively.

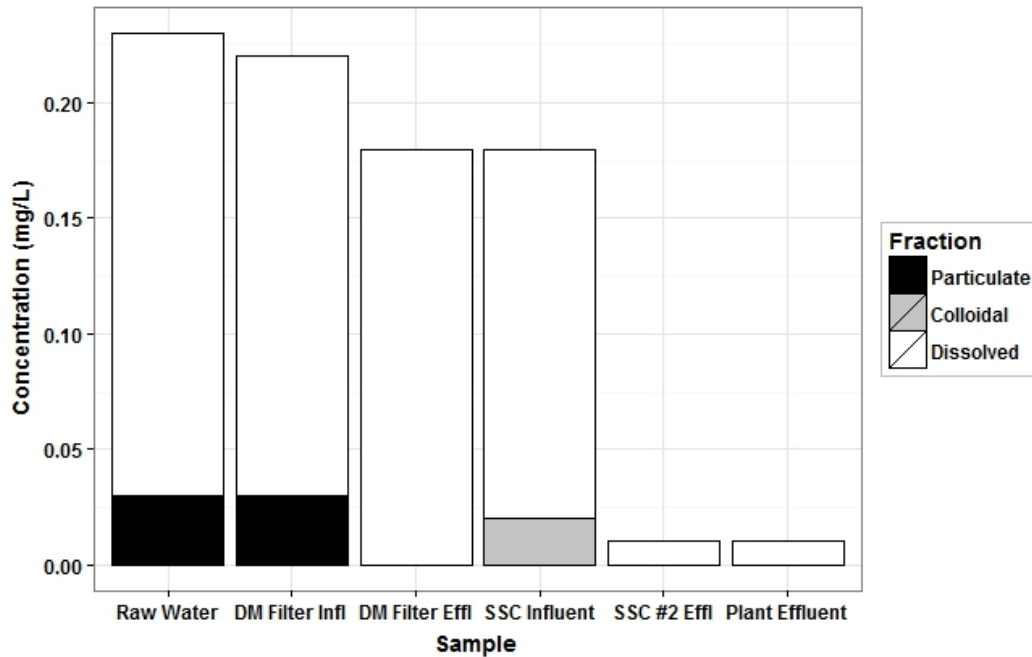


**Figure 4.6 Manganese fractionation across the plant on August 27th, 2013.**

#### 4.3.3.2 Contactor backwash

Due to the large size of the media in the contactors, the low influent turbidity, and lack of particle removal, as designed, the increase in head loss across the SSCs between backwashes was negligible. At lower plant flow rates (~ 350 gpm), SSC head loss was around 1.5 psi; at higher flows (~ 695 gpm), head loss was around 6 psi. Backwash was initially scheduled for every 2 weeks but changed to every 6 weeks because of no noticeable increase in head loss and continued effective Mn removal. A SSC backwash schedule of every 6 to 8 weeks with air scouring was adapted when it was determined from the mass balance (see below) that this did not adversely affect the oxide coating on the media. Similar to the DM filters, the three SSCs were backwashed sequentially, with down flow through two contactors used to backwash the third contactor at a HLR of 14 gpm/ft<sup>2</sup> achieving ~ 15% bed expansion. After backwashing of the SSCs is complete, a

10 minute contactor to waste period occurs to achieve stable Mn and chlorine levels prior to flow being directed to the distribution system.

After the initial few weeks of operation, recurring brief spikes in plant effluent turbidity but not in DM filter effluent turbidity were observed after the approximately daily DM filter backwash events. Investigations revealed that MnO<sub>x</sub> particles were released from the contactor media when valves were operated to switch flow from contactor to waste (at atmospheric pressure for discharge) to the distribution system (at ~ 65 psi). System data have shown that the raw water pump flow briefly drops to zero, then increases rapidly to the production set point (or beyond) as the variable speed pump drive responds to the change in discharge pressure. It is likely that the SSC media were slightly agitated during this rapid flow change, leading to release of MnO<sub>x</sub> particles. The impact was greater the longer the period of contactor operation without backwash. Operational changes have been made to minimize or eliminate the SSC effluent turbidity spike following the DM filter backwash and contactor to waste sequence.

#### **4.3.3.3 Mn mass balance**

Measurements of total Mn in digested composite contactor backwash samples were made to estimate the mass of Mn removed from the media during each backwash event. The mass of Mn removed by the contactors between backwash events was calculated using plant water production and average contactor influent and effluent Mn concentrations measured three times per week by utility personnel. Figure 4.7 compares the cumulative mass of Mn removed across the contactors and the estimated Mn mass in the contactor backwash for the cumulative volume of water treated from July 2013 to September 2015. Air scour was employed on December 23<sup>rd</sup>, 2013 (68 MG treated), prior

to taking the plant offline to complete construction, and again one year later on December 17<sup>th</sup>, 2014 (213 MG treated). One contactor (#1) was air-scoured for approximately 1 minute on March 2015 (249 MG treated) when the air scour was mistakenly left on. Air scouring was performed for all contactor backwash events starting on July 15<sup>th</sup> 2015 (310 MG treated).

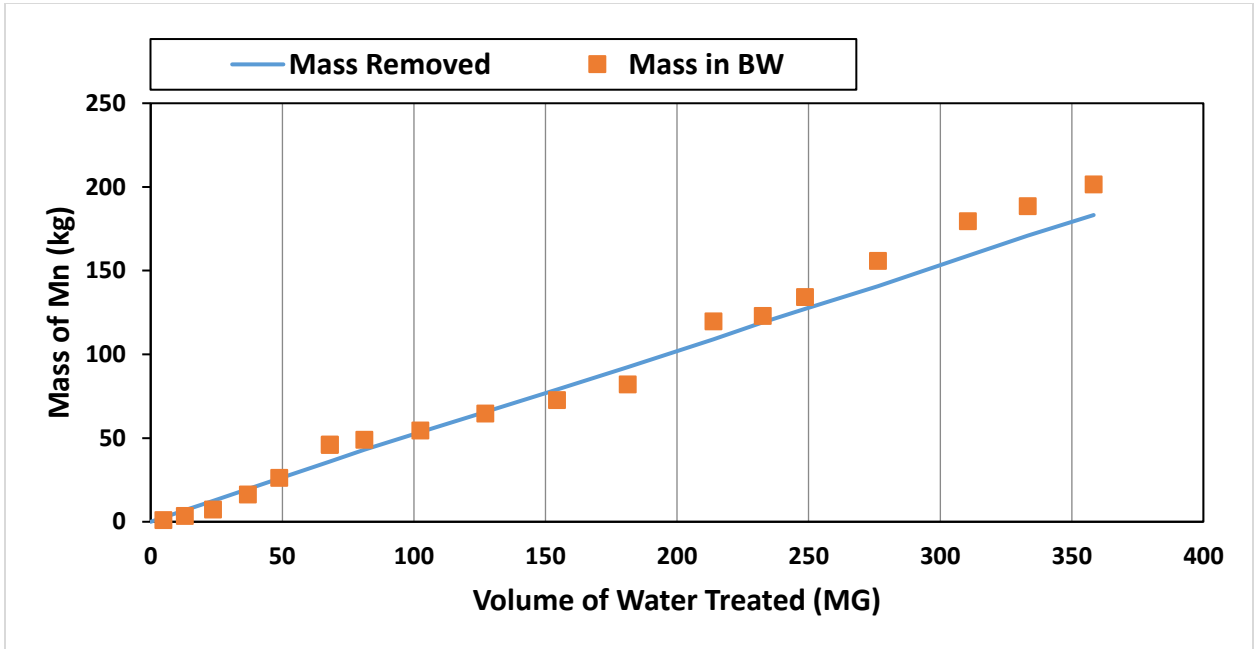


**Figure 4.7. Cumulative mass of Mn removed and in backwash from July 2013 to September 2015.**

The total amount of Mn in the waste contactor backwash for the period (201 kg) is similar to the total amount of Mn removed by the contactors (183 kg). The 10 % difference in the Mn removed by the contactors and the Mn in the backwash may be due the underestimation of contactor Mn removal and/or overestimation of the Mn mass in the backwash. The mass of Mn removed by the contactors was calculated using the plant water production and the decrease in Mn concentration across the contactors. This does not take into account Mn removed by the contactors during periods of plant operation

when the flow is wasted (e.g. during contactor-to-waste) and does not enter the distribution system.

#### **4.3.3.4 Media and backwash MnO<sub>x</sub> characterization**

Contact media MnO<sub>x</sub> coating levels were measured at the top of the media bed prior to plant startup in June 2013. Depth MnO<sub>x</sub> profiles were measured in February 2014 and September 2015 (Figure 4.8). Prior to startup, the MnO<sub>x</sub> coating levels at the top of the 3 contactors were 3.7, 3.4 and 2.5 mg Mn/g media; in February 2014 the coating levels 0-4 inches from the media surface were 7.0, 5.7, and 3.7 mg Mn/g media for contactors 1 to 3, respectively. In September 2015 the coating levels of the top 2 inches of the media beds were 5.2, 4.4, and 5.8 mg Mn/ g media, respectively, for the 3 contactors. The oxide coating levels at the top of the media increased significantly from the initial coating before start-up to the February 2014 sampling, while the levels in September 2015 were similar to or lower than the levels in February 2014. Contactor backwash, with and without air scouring, clearly did not remove all the MnO<sub>x</sub> coating, leaving levels sufficient for needed Mn(II) adsorption.

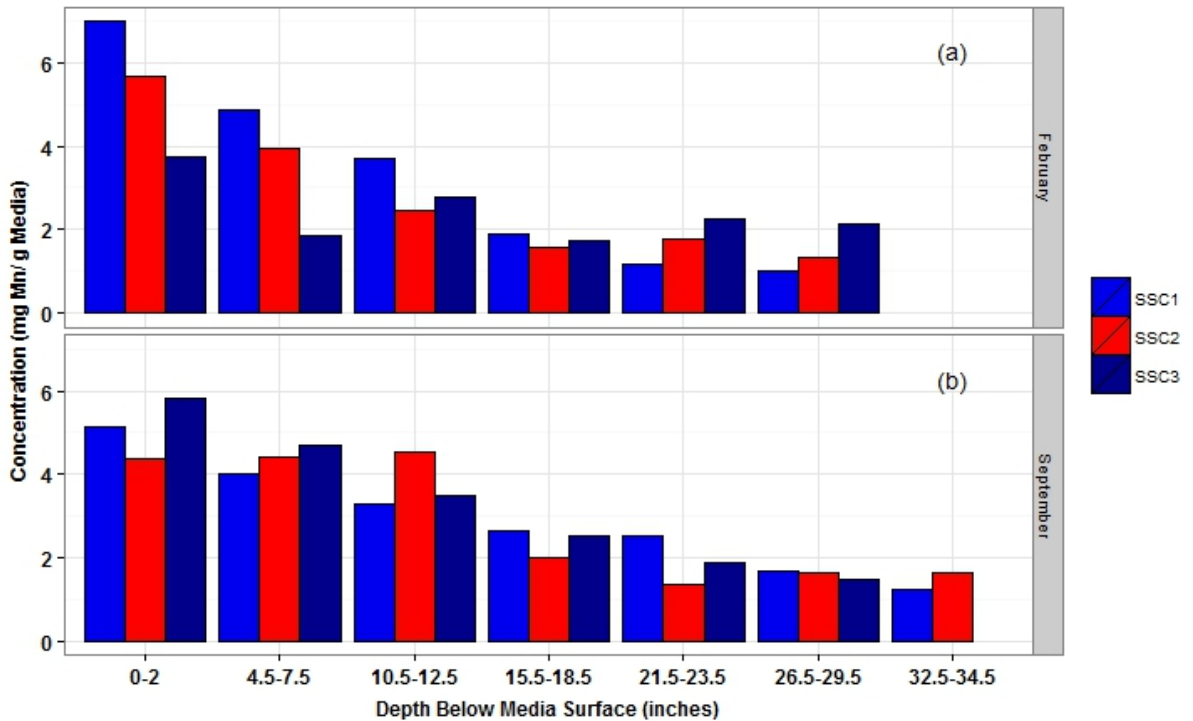
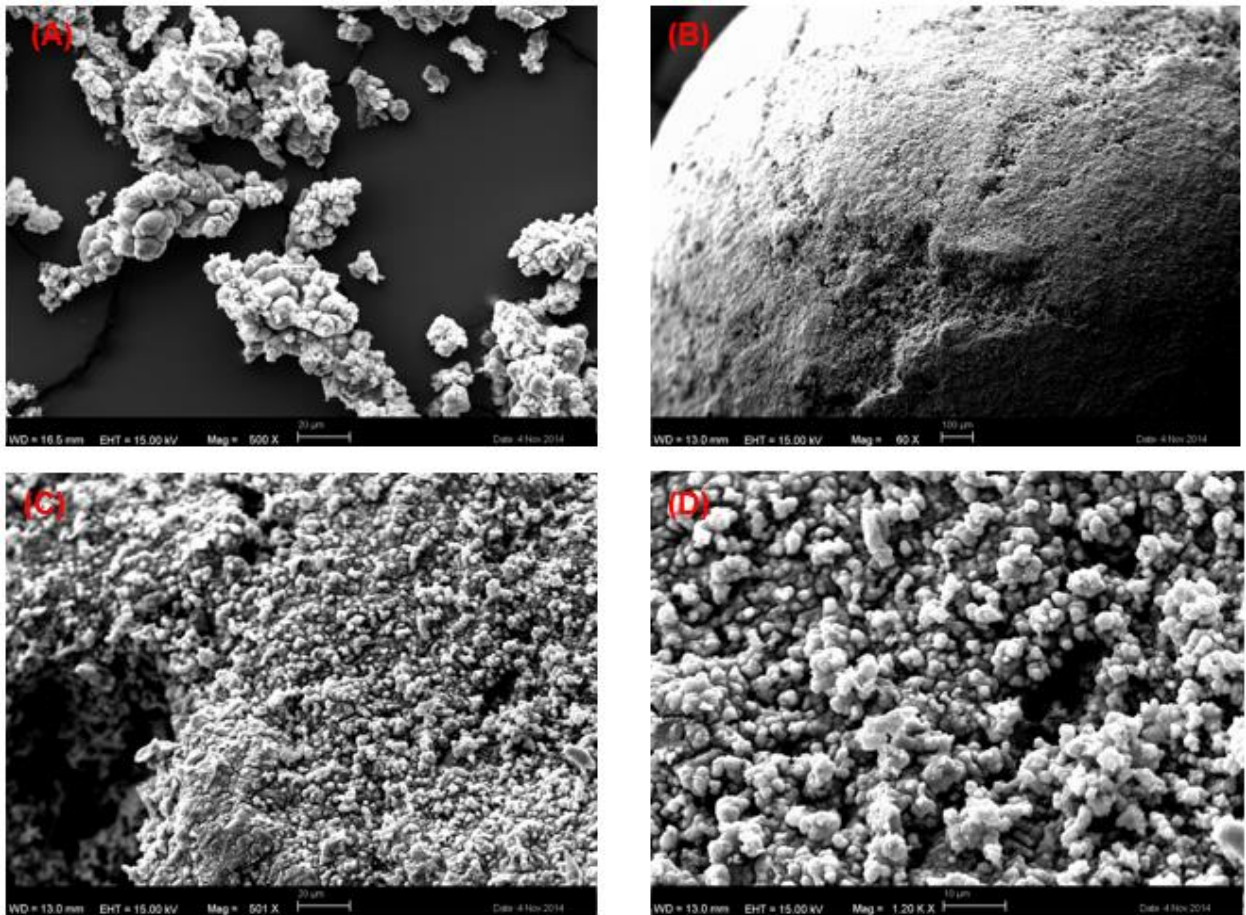


**Figure 4.8. SSC media MnO<sub>x</sub> coating depth profiles (a) February 2014 (b) September 2015.**

Depth profiles showed greater MnO<sub>x</sub> coating levels at the top of the media beds in all three contactors, at approximately 5.3 mg Mn/g media, which generally decreased with increasing depth to about 1.5 mg Mn/g media at depths below ~30 in. Profile measurements made in September 2015 indicated levels from 5.1 to 3.8 mg Mn/g media for the first 13 in, and lower levels of approximately 2.4 to 1.5 mg Mn/g media for the remainder of the bed. Similarly, measurements made in February 2014 ranged from 5.5 to 3.0 mg Mn/g media for the first 13 in, and 1.7 to 1.5 mg Mn/g media for the remainder of the bed. This profile is similar to data showing that the majority of Mn removal occurs towards the top of a fixed media bed in general (Islam et al. (2010); Knocke, Occiano and Hungate (1990)) and for the LHWTP lab and pilot studies conducted prior to full-scale

design (Chihoski (2012)). The contactor media profile for the mono media bed of Macrolite indicates that the media are not completely mixed by backwashing. This could reflect differences in media size and/or density such that some bed stratification is maintained after backwashing. In addition, available water depth above the media limits the extent of expansion and thus likely decreases the likelihood of full depth media mixing.

SEM images of the  $MnO_x$  coated Macrolite and  $MnO_x$  particles in waste contactor backwash samples are shown below. As expected, images of the waste backwash particles show clusters of particles similar to those observed on the surface of the  $MnO_x$  coated media.



**SEM images of (a) contactor backwash MnO<sub>x</sub> particles (magnification 500x), (b) through (d) MnO<sub>x</sub> coated Macrolite (magnifications of 60x, x500, and x1200 respectively).**

XPS analysis of the contactor backwash particles indicated that Mn in the MnO<sub>x</sub> was in the +4 oxidation state. This is in agreement with Cerrato et al. (2011) who showed that Mn removal by sorption and catalytic oxidation in the presence of chlorine resulted in MnO<sub>2(s)</sub>. X-ray diffraction analysis of the LHWTP backwash particles showed one small peak at a diffraction angle ( $2\theta$ ) of approximately  $36.5^\circ$  ( $2.43 \text{ \AA}$ ). The diffraction pattern with a low degree of crystallinity is similar to the amorphous  $\delta$ -MnO<sub>2</sub> characterized by Morgan and Stumm (1964) and Murray (1974).

#### **4.4 Broader Treatment Applications**

The second stage contactors for the Lantern Hill groundwater source were implemented specifically for the removal of dissolved Mn following removal of particles by upstream treatment processes. There are a number of situations where high HLR, coarse media, contactors for robust control of dissolved Mn in plant effluent may be an effective and optimal treatment alternative. For surface waters with seasonally elevated raw water Mn, use of second stage contactors with free chlorine allows for upstream biologically active media filtration, with decreased or eliminated raw water strong oxidant addition as the contactors function effectively for variable levels of dissolved Mn. Free chlorine use can achieve both Mn control and primary disinfection, as well as providing a distribution system disinfectant residual. For groundwaters with multiple contaminants, and especially natural organic matter, separation of processes for particle removal and dissolved Mn removal can provide a more effective and reliable treatment process as compared to single-stage approaches. Increasing health-based attention to control of Mn in finished water may lead to the need for Mn removal from sources that have relatively low levels of Mn. These sources may be amenable to removal by high rate coarse media contactors with lower energy demand as compared to traditional “greensand” type approaches using finer media.

#### **4.5 Conclusions**

Implementation of second stage contactors for removal of dissolved Mn(II) after first stage dual media filtration for particle removal was successful at the full-scale for a ground water source. The use of this approach was driven by the desire to use a single

pumping step from well to distribution system (necessitating direct filtration) and also to achieve both metals removal and DBP control. Delaying the addition of chlorine for catalytic Mn(II) oxidation until after particle and some NOM removal (by dual media filtration) resulted in a drastic decrease in plant effluent disinfection byproduct concentrations compared to levels from the original plant design. Effluent Mn concentrations of  $< 0.01$  mg/L were consistently achieved while maintaining low DBP concentrations. A mass balance showed that the Mn removed by the SSCs was reflected in the Mn present in the infrequent waste contactor backwash.

This study shows that SSCs can be implemented for Mn(II) removal at the full-scale. Use of SSCs would allow plants to practice post-filter chlorination (e.g. to enable use of bio-filtration or to control DBP formation) even if they experience seasonal elevated Mn(II) concentrations in the raw water.

## CHAPTER 5

### CONCLUSIONS

Mn(II) removal by sorption to MnO<sub>x</sub>-coated granular filter media and catalytic oxidation by free chlorine is commonly practiced in conventional surface water treatment or ground water treatment with the goal of Mn(II) removal. Previous studies showed that postponing chlorine addition from dual media filter influent to filter effluent could decrease DBP concentrations. This work aimed to determine the impact of MnO<sub>x</sub>, used for Mn(II) sorption, on DBP formation.

Results of batch experiments showed that the adsorption density of DOC to MnO<sub>x</sub> is low unless the ionic strength and/or divalent concentrations are high. There was no significant difference in measured TTHM and HAA<sub>5</sub> concentrations for samples with and without MnO<sub>x</sub> present in experiments using a synthetic water and experiments using surface water with low hardness. The DOC of the surface water did not exhibit NOM adsorption.

Documenting the decoupling of particle (and NOM) removal and Mn(II) removal at the full-scale provided evidence to support previous studies which showed that delaying chlorine addition until after NOM removal decreased TTHM and HAA<sub>5</sub> concentrations. SSCs were successful in removing Mn(II) (approximately 0.3 mg/L influent Mn) with effluent concentrations generally  $\leq 0.01$  mg/L, and allowed for the post-filter application of chlorine. However, it was not possible to determine at the full-scale whether the decrease in TTHM and HAA<sub>5</sub> formation was because of chlorination after NOM

removal, or less contact time with the  $\text{MnO}_x$ -coated surfaces in the presence of free chlorine.

Laboratory column experiments allowed for a more controlled examination of interactions with oxide-coated granular media. Instantaneous and 24-hour TTHM and  $\text{HAA}_5$  concentrations of laboratory column effluent were measured for samples where chlorine was added ahead of the column, and samples where chlorine was added to the column effluent. Post-column chlorinated instantaneous TTHM and  $\text{HAA}_5$  concentrations were lower than instantaneous concentrations of pre-column chlorinated samples. The 24-hour concentrations of pre-column chlorinated and post-column chlorinated samples, however, were not significantly different. Influent and effluent instantaneous and 24-hour TTHM and  $\text{HAA}_5$  concentrations of two  $\text{MnO}_x$ -coated media reactors at two full-scale plants were also analyzed. It was concluded that exposure to a  $\text{MnO}_x$ -coated anthracite surface did not increase the TTHM and  $\text{HAA}_5$  formation potential of the water, but rather the increase in instantaneous TTHM and  $\text{HAA}_5$  concentrations from influent to effluent was a function of increased reaction time (the residence time of the reactor).

The results of studies undertaken suggest that contact with a  $\text{MnO}_x$ -coated surface during treatment did not increase TTHM and  $\text{HAA}_5$  formation for different waters, and in the pH range of ~5 to ~8. These findings have significant implications for drinking water treatment. If water NOM characteristics and concentrations make pre-filter chlorination undesirable, SSCs present an alternative for Mn(II) removal after filtration by WTPs.

Additional research is needed to gain a better understanding of favorable source water NOM characteristic and water chemistry for NOM transformation by  $\text{MnO}_x$  in drinking water treatment. Within the complex context of drinking water treatment, where

the NOM composition depends on a variety of watershed characteristics (climate, geology, and hydrology, land use, etc.), this may be challenging. The increasing use of novel analytical tools to drinking water treatment, and development of methods with greater sensitivity and lower limits of detection, will hopefully further elucidate NOM and  $\text{MnO}_x$  interactions in drinking water systems.

APPENDIX A

SUPPLEMENTAL DATA FOR CHAPTER 2

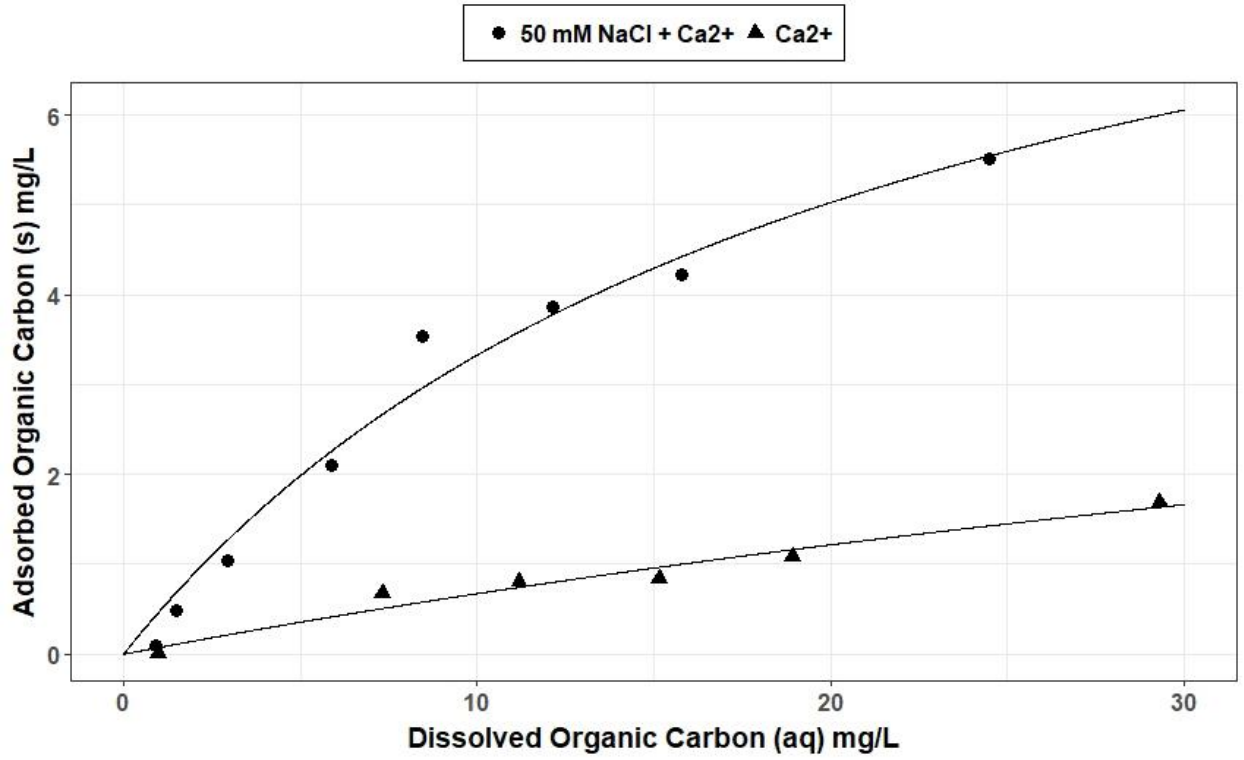


Figure A.1. Adsorbed and solution organic carbon concentrations. Reaction time 24 hours, pH of 6.1, at 20 °C, 0.5 mM Ca<sup>2+</sup>.

**APPENDIX B**

**SUPPLEMENTAL DATA FOR CHAPTER 3**

**Table B.1: Column run water quality parameters.**

	Time (min)	UV <sub>254</sub> Abs (cm <sup>-1</sup> )	Turbidity (NTU)	Cl <sub>2</sub> Residual (mg/L)	Total Mn (HACH) (mg/L)
Pre-Cl <sub>2</sub> , No Media, Settled Water	5	0.037	0.230	1.21	0.34
	10	0.038	0.258	1.37	0.33
Pre-Cl <sub>2</sub> , Coated Media, DI Water	5	0.007	0.212	2.66	0.03
	10	0.005	0.191	3.00	0.01
Pre-Cl <sub>2</sub> , Coated Media, Settled Water	2	0.036	0.231	0.69	0.04
	10	0.035	0.191	1.11	0.04
	16	0.035	0.161	1.02	0.04
	22	0.037	0.190	1.01	0.06
	30	0.035	0.175	0.98	0.07
Pre-Cl <sub>2</sub> , Uncoated Media, DI Water	5	0.005	0.210	2.70	< 0.01
	10	0.008	0.180	2.85	< 0.01
Pre-Cl <sub>2</sub> , Uncoated Media, Settled Water	2	0.039	0.237	1.35	0.28
	10	0.045	0.159	1.39	0.25
	16	0.036	0.201	1.36	0.24
	22	0.035	0.351	1.29	0.22
	30	0.037	0.240	1.38	0.21
Post-Cl <sub>2</sub> , Coated Media, DI Water	7	0.003	0.207	2.70	< 0.01
	17	0.003	0.240	2.30	< 0.01
Post-Cl <sub>2</sub> , Coated Media, Settled Water	4	0.036	0.135	1.10	0.05
	13	0.037	0.214	1.67	0.04
	18	0.038	0.256	1.94	0.06
	27	0.038	0.238	1.55	0.05
	30	0.040	0.171	1.45	0.08
	63	0.041	0.253	1.46	0.09
	76	0.042	0.156	1.43	0.10

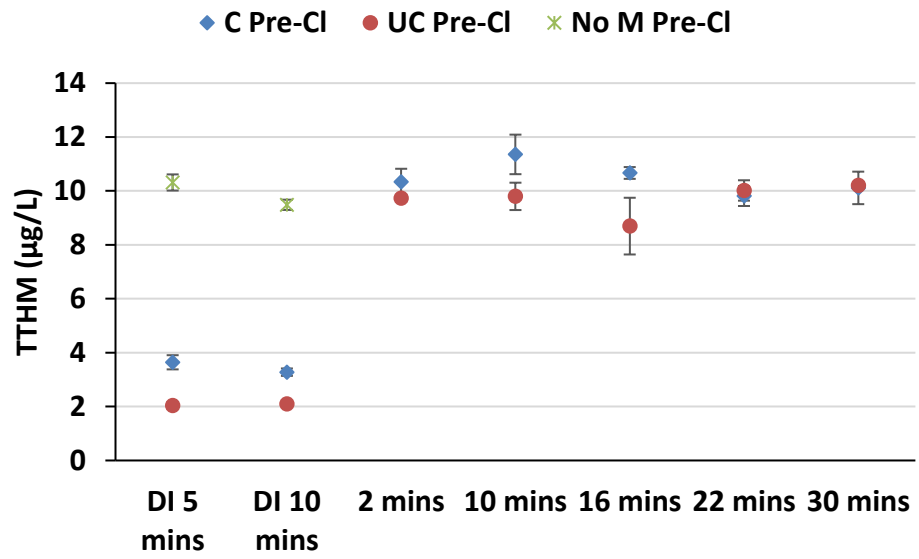


**Figure B.1. Instantaneous TTHM concentrations.**

## BIBLIOGRAPHY

- APHA, AWWA, WEF, 1998. Standard Methods for the Examination of Water and Wastewater. APHA, AWWA, and WEF, Washington, D.C.
- Bazilio, A. A., Kaminski, G. S., Larson, Y., Mai, X., Tobiason, J. E., 2016. Full-Scale Implementation of a Second-Stage Contactor for Manganese Removal. *J. Am. Water Works Assoc.*, 108 (12), EE 606. <http://dx.doi.org/10.5942/jawwa.2016.108.0184>
- Brandhuber, P.; Clark, S.; Knocke, W.; & Tobiason, J., 2013. Guidance for the Treatment of Manganese. Water Research Foundation, Denver.
- Brophy, K. S., Weinberg, H. S., Singer, P. C., 2000. Quantification of nine haloacetic acids using gas chromatography with electron capture detection. ACS Symposium Series 761, 343-355.
- Brown, M., 2006. The Relationship between Pre-filter Chlorine Addition and Enhanced Disinfection Byproduct Formation. Master's Project Report, Department of Civil and Environmental Engineering, University of Massachusetts, Amherst, MA.
- Carlson, K.H.; Knocke, W.R.; & Gertig, K.R., 1997. Optimizing Treatment Through Fe and Mn Fractionation. *J. Am. Water Works Assoc.*, 89:4:162.
- Cerrato, J. M., Knocke, W. R., Hochella Jr, M. F., Dietrich, A. M., Jones, A., Cromer, T. F., 2011. Application of XPS and Solution Chemistry Analyses to Investigate Soluble Manganese Removal by MnO<sub>x</sub> (s)-Coated Media. *Environ. Sci. Technol.*, 45 (23), 10068-10074.
- Cerrato, J. M., Hochella Jr, M. F., Knocke, W. R., Dietrich, A. M., Cromer, T. F., 2010. Use of XPS to identify the oxidation state of Mn in solid surfaces of filtration media oxide samples from drinking water treatment plants. *Environ. Sci. Technol.*, 44 (15), 5881-5886.
- Chihoski, J., 2012. Evaluation of Second-Stage Contactor Media for Manganese Removal. Master's Project Report, Department of Civil and Environmental Engineering, University of Massachusetts, Amherst, MA.
- Corbin, M. J., Reckhow, D. A., Tobiason, J. E., Dunn, H. J., Kaminski, G. S., 2003. Controlling DBPs by delaying chlorine addition until after filtration. *J New England Water Works Assoc.* 117 (4), 243-251.
- Davis, J. A. and Gloor, R., 1981. Adsorption of dissolved organics in lake water by aluminum oxide. Effect of molecular weight. *Environ. Sci. Technol.*, 15 (10), 1223-1229.
- Day, G. M., Hart, B. T., McKelvie, I. D., Beckett, R., 1994. Adsorption of natural organic matter onto goethite. *Colloids Surfaces A: Physicochem. Eng. Aspects*, 89 (1), 1-13.

- Gabelich, C. J., Geringer, F. W., Knocke, W. R., Lee, C. C., 2006. Sequential manganese desorption and sequestration in anthracite coal and silica sand filter media. *J. Am. Water Works Assoc.*, 98 (5), 116-127.
- Gallard, H., Allard, S., Nicolau, R., Von Gunten, U., Croué, J. P., 2009. Formation of iodinated organic compounds by oxidation of iodide-containing waters with manganese dioxide. *Environ. Sci. Technol.*, 43 (18), 7003-7009.
- Gu, B., Schmitt, J., Chen, Z., Liang, L., McCarthy, J. F. 1994. Adsorption and desorption of natural organic matter on iron oxide: mechanisms and models. *Environ. Sci. Technol.*, 28 (1), 38-46.
- Health Canada, 2016. Manganese in Drinking Water: Document for Public Consultation. Federal-Provincial-Territorial Committee on Drinking Water, Ottawa, Ontario.
- Healy, T. W., Herring, A., Fuerstenau, D., 1966. The effect of crystal structure on the surface properties of a series of manganese dioxides. *J. Colloid Interface Sci.*, 21 (4), 435-444.
- Islam, A. A., Goodwill, J. E., Bouchard, R., Tobiason, J. E., Knocke, W. R., 2010. Characterization of filter media MnO<sub>x</sub> (s) surfaces and Mn removal capability. *J. Am. Water Works Assoc.*, 102 (9), 71-83.
- Johnson, K., Purvis, G., Lopez-Capel, E., Peacock, C., Gray, N., Wagner, T., März, C., Bowen, L., Ojeda, J., Finlay, N., 2015. Towards a mechanistic understanding of carbon stabilization in manganese oxides. *Nature Communications*, 6, p. 7628. doi:10.1038/ncomms8628.
- Knocke, W. R., Zuravnsky, L., Little, J. C., Tobiason, J. E., 2010. Adsorptive contactors for removal of soluble manganese during drinking water treatment. *J. Am. Water Works Assoc.*, 102 (8), 64-75.
- Knocke, W. R., Occiano, S. C., Hungate, R. 1991. Removal of soluble manganese by oxide-coated filter media: sorption rate and removal mechanism issues. *J. Am. Water Works Assoc.*, 83 (8) 64-69.
- Knocke, W. R., Occiano, S., Hungate, R., 1990. Removal of soluble manganese from water by oxide-coated filter media. AWWA Research Foundation and the American Water Works Association, Denver.
- Knocke, W. R., Ramon, J. R., Thompson, C. P., 1988. Soluble manganese removal on oxide-coated filter media. *J. Am. Water Works Assoc.*, 80 (12), 65-70.
- Knocke, W. R., Hoehn, R. C., Sinsabaugh, R. L., 1987. Using alternative oxidants to remove dissolved manganese from waters laden with organics. *J. Am. Water Works Assoc.*, 79 (3), 75-79.

- Kohl, P. M. and Medlar, S. J., 2006. Occurrence of Manganese in Drinking Water and Manganese Control. Water Research Foundation, Denver.
- Korshin, G. V., Benjamin, M. M., Sletten, R. S., 1997. Adsorption of natural organic matter (NOM) on iron oxide: Effects on NOM composition and formation of organo-halide compounds during chlorination. *Water Res.*, 31 (7), 1643-1650.
- Liu, R., Liu, H., Qiang, Z., Qu, J., Li, G., Wang, D., 2009. Effects of calcium ions on surface characteristics and adsorptive properties of hydrous manganese dioxide. *J. Colloid Interface Sci.*, 331 (2), 275-280.
- Merkle, P. B., Knocke, W., Gallagher, D., Junta-Rosso, J., Solberg, T., 1996. Characterizing filter media mineral coatings. *J. Am. Water Works Assoc.*, 88 (12), 62.
- Morgan, J. J. and Stumm, W., 1964. Colloid-chemical properties of manganese dioxide. *J. Colloid Interface Sci.*, 19 (4), 347-359.
- Murray, J. W., 1975. The interaction of metal ions at the manganese dioxide-solution interface. *Geochim. Cosmochim. Acta*, 39 (4), 505-519.
- Murray, J. W., 1974. The surface chemistry of hydrous manganese dioxide. *J. Colloid Interface Sci.*, 46 (3), 357-371.
- Pham, M., 2010. Two-Stage Filtration to Control Manganese and DBPs at the Lantern Hill Water Treatment Plant. Master's Project Report, Department of Civil and Environmental Engineering, University of Massachusetts, Amherst, MA.
- Richardson, S. D., Plewa, M. J., Wagner, E. D., Schoeny, R., DeMarini, D. M., 2007. Occurrence, genotoxicity, and carcinogenicity of regulated and emerging disinfection by-products in drinking water: a review and roadmap for research. *Mutat. Res.*, 636 (1-3), 178-242.
- Richardson, S. D., 2003. Disinfection by-products and other emerging contaminants in drinking water. *TrAC Trends Anal. Chem.*, 22 (10), 666-684.
- Russell, J., 2008. Control of Manganese, Iron, and Disinfection By-Products for the Mystic Connecticut Water System. Master's Project Report, Department of Civil and Environmental Engineering, University of Massachusetts, Amherst, MA.
- Sly, L. I., Hodgkinson, M. C., Arunpairojana, V., 1990. Deposition of manganese in a drinking water distribution system. *Appl. Environ. Microbiol.*, 56 (3), 628-639.
- Stone, A. T. and Morgan, J. J., 1984a. Reduction and dissolution of manganese(III) and manganese(IV) oxides by organics: 1. Reaction with hydroquinone. *Environ. Sci. Technol.*, 18 (6), 450-456.

- Stone, A. T. and Morgan, J. J., 1984b. Reduction and dissolution of manganese(III) and manganese(IV) oxides by organics: 2. Survey of the reactivity of organics. *Environ. Sci. Technol.*, 18 (8), 617-624.
- Thurman, E. M., 1985. Organic Geochemistry of Natural Waters. Nijhoff, Boston.
- Tipping, E. and Heaton, M., 1983. The adsorption of aquatic humic substances by two oxides of manganese. *Geochim. Cosmochim. Acta*, 47 (8), 1393-1397.
- Tipping, E., 1981. Adsorption by goethite ( $\alpha$ -FeOOH) of humic substances from three different lakes. *Chem. Geology*, 33 (1), 81-89.
- Tipping, E. and Cooke, D., 1982. The effects of adsorbed humic substances on the surface charge of goethite ( $\alpha$ -FeOOH) in freshwaters. *Geochim. Cosmochim. Acta*, 46 (1), 75-80.
- Tipping, E., 1986. Some aspects of the interactions between particulate oxides and aquatic humic substances. *Marine Chem.*, 18 (2-4), 161-169.
- Tobiason, J. E., Bazilio, A., Goodwill, J., Mai, X., Nguyen, C., 2016. Manganese Removal from Drinking Water Sources. *Curr. Pollution Rep.*, 2 (3), 168-177. <https://doi.org/10.1007/s40726-016-0036-2>
- Tobiason, J. E., Islam, A. A., Goodwill, J. E., Hargette, P. H., Bouchard, R., Zuravnsky, L., 2008. Characterization and Performance of Filter Media for Manganese Control. AWWA Research Foundation, Denver.
- Ulrich, H. J. and Stone, A. T. 1989. The oxidation of chlorophenols adsorbed to manganese oxide surfaces. *Environ. Sci. Technol.*, 23 (4), 421-428.
- US Agency for Toxic Substances and Disease Registry, 2012. Toxicological Profile for Manganese.
- USEPA, 2006. National Primary Drinking Water Regulations: Stage 2 Disinfectants and Disinfection Byproducts Rule. 40 CFR Parts 9, 141, and 142.
- USEPA, 2004. Drinking Water Health Advisory for Manganese. USEPA Health and Ecological Criteria Division, Office of Science and Technology, Office of Water, Washington, DC.
- USEPA, 1995. Determination of Haloacetic Acids and Dalapon in Drinking Water by Liquid-Liquid Extration, Derivatization and Gas Chromatography with Electron Capture Detection. USEPA, Cincinnati, OH.
- USEPA, 1992. Secondary Drinking Water Regulations: Guidance for Nuisance Chemicals. EPA-810/K-92-001.

USEPA, 1990. Determination of Chlorination Disinfection Byproducts, Chlorinated Solvents, and Halogenated Pesticides/Herbicides in Drinking Water by Liquid-Liquid Extraction and Gas Chromatography with Electron-Capture Detection. USEPA, Cincinnati, OH.

Wang, Y. and Stone, A. T., 2006a. The citric acid–Mn<sup>III, IV</sup> O<sub>2</sub>(birnessite) reaction. Electron transfer, complex formation, and autocatalytic feedback. *Geochim. Cosmochim. Acta*, 70 (17), 4463-4476.

Wang, Y. and Stone, A. T., 2006b. Reaction of Mn<sup>III,IV</sup> (hydr)oxides with oxalic acid, glyoxylic acid, phosphonoformic acid, and structurally-related organic compounds. *Geochim. Cosmochim. Acta*, 70 (17), 4477-4490.

Weng, L., Van Riemsdijk, W. H., Koopal, L. K., Hiemstra, T. 2006. Adsorption of humic substances on goethite: comparison between humic acids and fulvic acids. *Environ. Sci. Technol.*, 40 (24), 7494-7500.